Supplementary online material for :

Weight Consistency Specifies Regularities of Macaque Cortical Networks

Running title: **Cortical Connectivity Profiles**

Authors:

N. T. Markov[a,b,1], P. Misery [a,b,1], A. Falchier[a,b,e], C. Lamy[a,b], J. Vezoli[a,b], R. Quilodran[a,b], P. Giroud[a,b], M. A. Gariel[a,b], M. M. Ercsey-Ravasz[c], L. J. Pilaz[a,b], C. Huissoud[a,b], P. Barone[a,b,e], C. Dehay[a,b], Z. Toroczkai[c], D. C. Van Essen[d], H. Kennedy[a,b,2,3], K. Knoblauch[a,b,2,3]

CONTENT:

Technical considerations. The tracers used in this study (FsB and DY) have two important advantages with respect to other tracers.

Firstly, these dyes do not show secondary uptake. This is indicated by the pattern of interhemispheric labeling following injections in either area V1 and V2. It is known that area V2 on the V1/V2 border shows strong inter-hemispheric connectivity while area V1 lacks callosal connections (Dehay et al. 1986; Dehay et al. 1988). Injections in area V2 fail to label neurons in the contralateral area V1 off the V1/V2 border, similarly injections in area V1 fail to label any neurons in the contralateral hemisphere (this study). This last result is actually very convincing, because the density of the ipsilateral V2 labeling is extremely high (V2 projections to V1 are one of the highest densities of intra-cortical connections, so that one would expect some of the contralateral neurons that target the ipsilateral V2 to be labeled. They are not. One possible although not convincing objection to the observation that injection in V1 fails to label contralateral V2 is that it is a long distance connection. One can counter this with the observation that paracentral V4 is well known to have no input from area V1, despite a strong input from area V2. Again, given the strong V2->V1 projection, if transynaptic labeling were to occur then one would find back labeled cells in V1 following large injections of DY and FsB in V4. This is not the case. Finally, here and elsewhere, we have shown that despite the intrinsic labeling being very dense, it has a sharp drop off over two or three millimeters. If there were any transynaptic labeling at all this could not be the case. These results, and numerous unpublished observations, mean that following their retrograde transport to the source area, these tracers are not released and picked up by neurons or by afferents to the source area in quantities sufficient to lead to secondary labeling (see discussion (Bullier et al. 1984a, 1984b)).

Secondly there are particular concerns about correctly identifying the region where tracer is taken up at the injection site. In our earlier studies we found that optimal labeling with these dyes requires that a crystalline bolus of tracer be deposited in the cortex, as can be achieved when the injection is made parallel to the surface in a site spanning several millimeters and the tracer injected slowly while withdrawing the needle (Bullier et al. 1984a; Kennedy and Bullier 1985; Perkel et al. 1986). This leads to relatively large injections sites, which though increasing the workload (more labeled neurons requires more person-months in charting their location) are necessary for good quality labeling. Relatively large injection sites are also necessary to ensure that they are sufficiently large to overcome possible heterogeneity in the injected area, as speculated by Scannell; small injections could lead to between-injection variability (MacNeil et al. 1997; Scannell et al. 2000).

The uptake zones of the tracers used in the present study are restricted to the near vicinity of the needle track, which is important for allowing counts of labeled intrinsic neurons and location of the injection to a particular cortical area. The characterization of the uptake zone of these tracers is

supported by numerous observations. For instance, after similar injections to those used in the present study, labeled intrinsic neurons have highly characteristic distributions. Around the needle tract, the spread of labeled neurons in layers 2/3 and 5/6 are relatively extensive while labeled neurons in layer 4 extend less that 400μm from the needle tract (Bullier and Kennedy 1983; Barone et al. 2000). These differences in the distances of labeled neurons reflect the known differences in the projection distances of neurons in the different cortical layers, hence the projection distances in layer 4 are considerably shorter than in the supra- and infragranular layers (see discussion in (Bullier and Kennedy 1983). Another indication of the extent of the uptake zone has been obtained by examining the topography of the projection of the LGN on to area V1 as revealed with these dyes. The projection of the LGN on to area V1 is highly point to point. Hence injections of either FsB or DY lead to a narrow column of cells spanning the layers of the LGN. Bullier and Kennedy (Bullier and Kennedy 1987) made paired injections (i.e. injection of FsB and DY) in area V1 with varying separations. When the pair of tracers were injected in area V1 with a separation of 3 mm, the columns of retrogradely labeled cells are separate in the LGN. Reducing the inter-injection distance, reduced the separation of the two populations of labeled neurons. It is only when the two injection sites were separated by 1.9 mm that the populations of labeled neurons in LGN began to show overlap and double labeled neurons were obtained (Bullier and Kennedy 1987). Given that the axonal arbor of the LGN neurons in the cortex span 400μm, this suggests that the uptake zone corresponds to a zone only marginally larger than the needle tract (Bullier et al. 1984b; Kennedy and Bullier 1985; Perkel et al. 1986; Conde 1987).

Because cortical afferents terminate in all layers it is advantageous that injection sites involve layers 6 to 1. Armed with our knowledge of the uptake zone at the injection site, we are able to identify those uptake zones that significantly involve the underlying white matter of the injected target area. Uptake zones that involve the white matter could lead to labeling of projections outside of the area injected and therefore may contribute to FLN variability. The injections in the present study were restricted to the cortical gray matter except for case 101LH **(see fig S2E)** that showed some white mater involvement.

There are ethical reasons for not discarding an injection without due cause and several arguments in favor of retaining case 101LH. Firstly, the distribution of FLN values overlap with the values of the other two injections in area V2 and differ from those obtained following injections in V1 **(Fig S8)**. Secondly, when injections are restricted to the white matter, we found that while subcortical structures were labeled, there was either an absence of cortical labeling or uniquely labeling of the corticofugal neurons. In the case of LH101 white matter encroachment does not appear to influence labeling in area V1 where quantification of the laminar distribution of the labeling gives a value of 75% labeled supranular layer neurons, similar to that found after both of the 2 injections in V2 used in this study (data not shown). A further consideration in favor of retaining this injection is the pattern of

labeling in the LGN. Compared to V1, injections in area V2 label relatively fewer cells in the LGN that are chiefly located in between the LGN layers (Bullier and Kennedy 1983).

Bibliography to technical considerations:

Barone P, Batardiere A, Knoblauch K, Kennedy H. 2000. Laminar distribution of neurons in extrastriate areas projecting to visual areas V1 and V4 correlates with the hierarchical rank and indicates the operation of a distance rule. J Neurosci. 20: 3263-3281.

Bullier J, Kennedy H. 1983. Projection of the lateral geniculate nucleus onto cortical area V2 in the macaque monkey. Exp Brain Res. 53: 168-172.

Bullier J, Kennedy H. 1987. Axonal bifurcation in the visual system. Trends Neurosci. 10: 205-210.

Bullier J, Kennedy H, Salinger W. 1984a. Bifurcation of subcortical afferents to visual areas 17,18 and 19 in the cat cortex. J Comp Neurol. 228: 309-328.

Bullier J, Kennedy H, Salinger W. 1984b. Branching and laminar origin of projections between visual cortical areas in the cat. J Comp Neurol. 228: 329-341.

Conde F. 1987. Further studies on the use of the fluorescent tracers fast blue and diamidino yellow: effective uptake area and cellular storage sites. J Neurosci Methods. 21: 31-43.

Dehay C, Kennedy H, Bullier J. 1986. Callosal connectivity of areas V1 and V2 in the newborn monkey. J Comp Neurol. 254: 20-33.

Dehay C, Kennedy H, Bullier J, Berland M. 1988. Absence of interhemispheric connections of area 17 during development in the monkey. Nature. 331: 348-350.

Kennedy H, Bullier J. 1985. A double-labeling investigation of the afferent connectivity to cortical areas V1 and V2 of the macaque monkey. J Neurosci. 5: 2815-2830.

MacNeil MA, Lomber SG, Payne BR. 1997. Thalamic and cortical projections to middle suprasylvian cortex of cats: constancy and variation. Exp Brain Res. 114: 24-32.

Perkel DJ, Bullier J, Kennedy H. 1986. Topography of the afferent connectivity of area 17 in the macaque monkey: a double-labelling study. J Comp Neurol. 253: 374-402.

Scannell JW, Grant S, Payne BR, Baddeley R. 2000. On variability in the density of corticocortical and thalamocortical connections. Philos Trans R Soc Lond B Biol Sci. 355: 21-35.

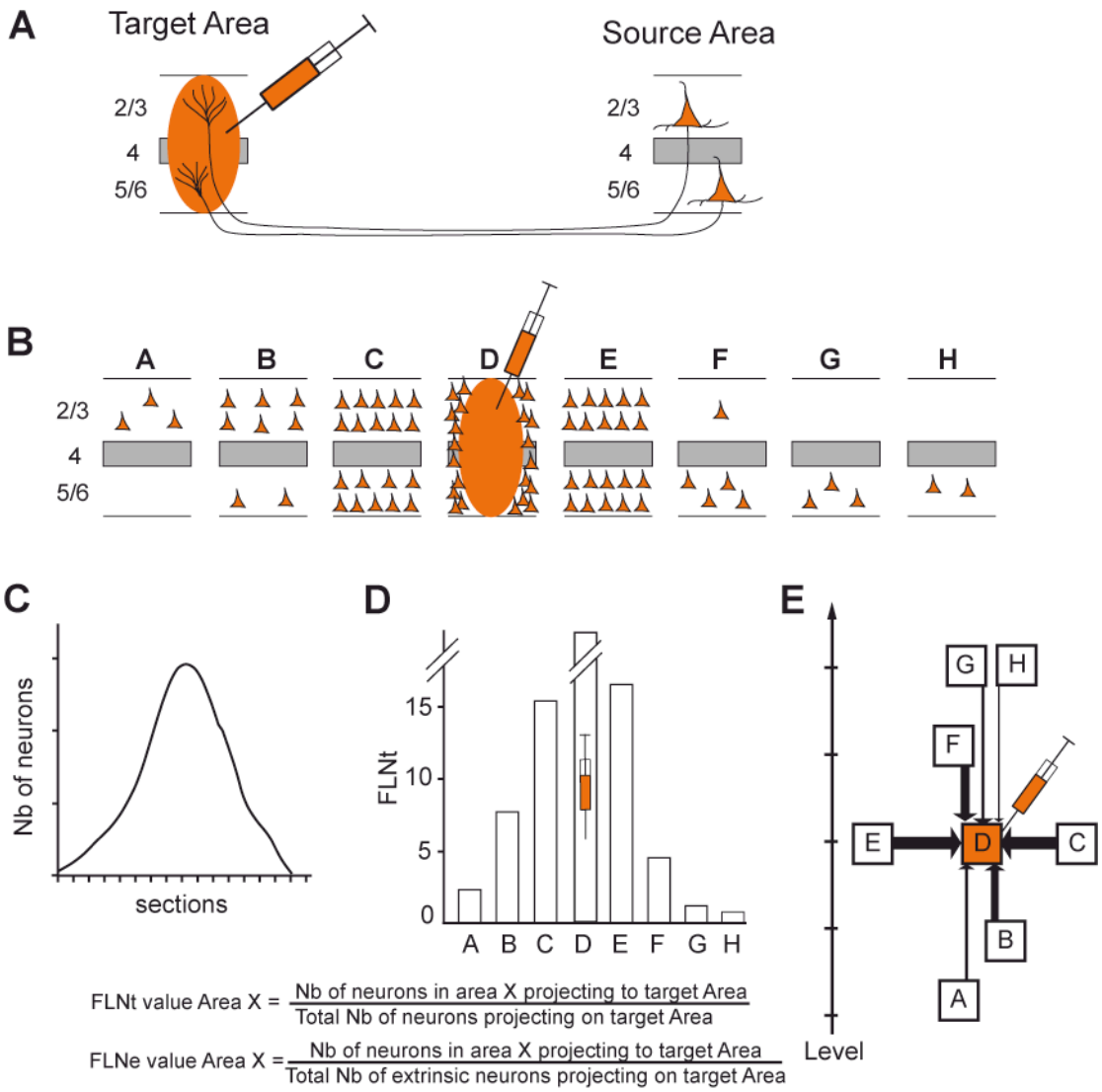

Fig S1: Track tracing procedures and calculation of FLN. A: The tracers Diamidino Yellow and Fast Blue used in this study are picked up at the axon terminal and transported retrogradely to the cell body (Bullier et al., 1984a; Kuypers et al., 1980). The high sensitivity of these retrograde tracers means that they have repeatedly been used to reveal previously unknown pathways (Barone et al., 2000; Bullier and Kennedy, 1983; Falchier et al., 2002; Kennedy and Bullier, 1985; Kennedy et al., 1989; Perkel et al., 1986). When injections of these tracers in the target area are large, made in a stereotypic fashion and restricted to the cortical gray matter, the labeled neurons in the source area have highly reproducible distributions as shown previously (Barone et al., 2000; Barone et al., 1995; Vezoli et al., 2004). In this way, injections of these tracers in the target area reveal the population of neurons in the source area that project to the injection site in the target area. **B**: Injection in target area D labels neurons in source areas A to C and E to H as well as in the target area D. **C**: Counts of neurons in successive sections from each area are used to generate a density profile. The smooth curve of the density profile means that the projection zone has been appropriately sampled. **D**: Total surface under the curve of the density profile makes it possible to obtain neuron numbers for each area. **E**: Neuron numbers in D are used to calculate the FLN values. The FLN percentage is generated as the ratio of the sum of retrogradely labeled neurons labeled in a given source structure over the sum of retrogradely labeled neurons in the brain.

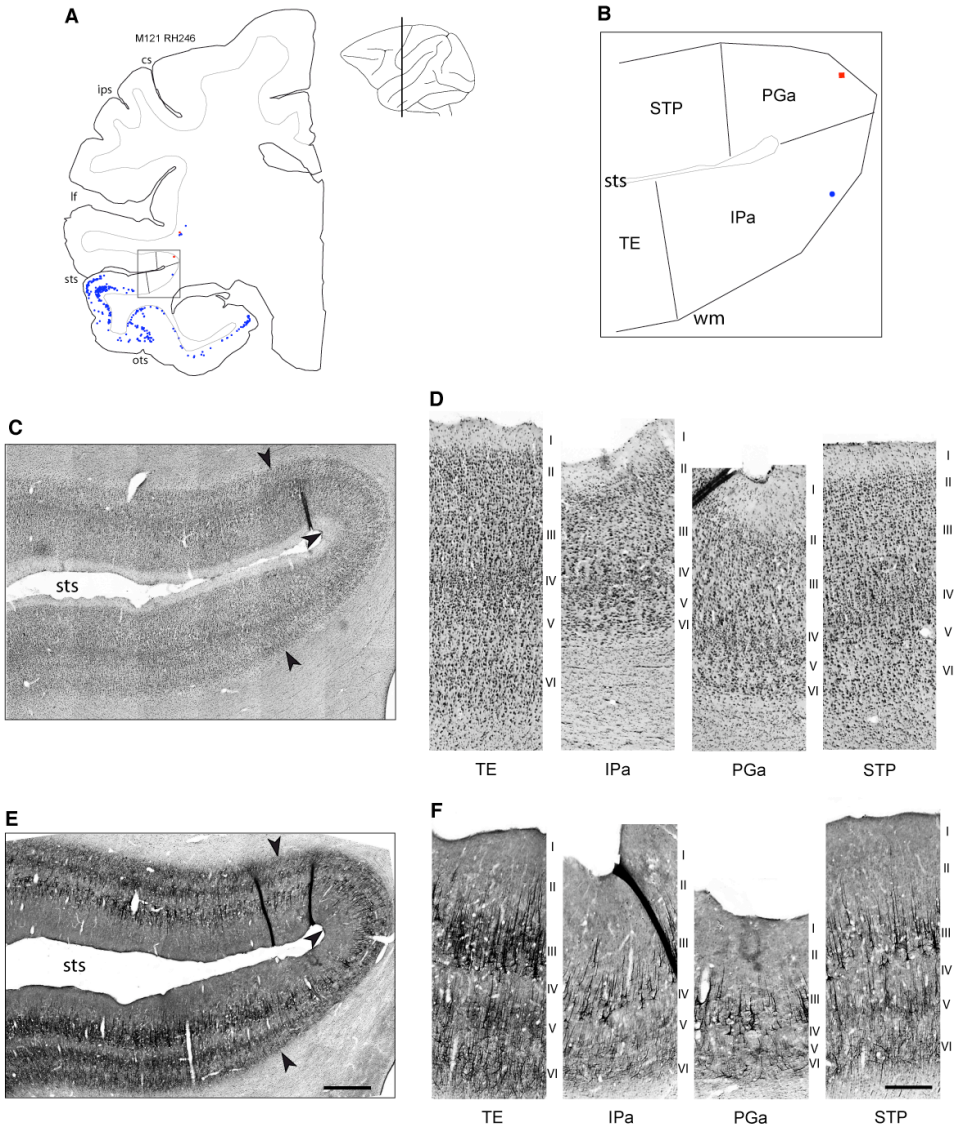

Fig S2. Illustration of the projection from IPa and PGa on to area V1. A: We identify areas IPa and PGa as occupying the fundus of the superior temporal sulcus anterior to area FST. After V1 injections we systematically observe sparse largely distributed label in these areas. B: Drawing of a cortical hemisphere with indication of the section level of the plot map shown in figure A and a magnification of the fundus of the STS where labeled neurons are found. Although the number of neurons per section is small the label is present over many sections and is found consistently across animals. C and D: Low and high magnification micrographs of Nissl stain of the section in A. The cytoarchitectonic criteria that we use have been previously defined by others (Seltzer and Pandya 1978). The cytoarchitectonic of area TE shows large pyramidal cells in layer 3c the layers 5 and 6 are better defined and more easily identified as compared to these of area IPa. Area IPa occupies the fundus of the STS on the ventral side it has large darkly stained pyramid cells in both layers 3 and 5. Area PGa has a prominent layer 2 with cells forming clustered groups STP has a very well defined layer 4 and very homogenous cell density between layers 5 and 6 which makes them difficult to distinguish but presents a segmentation characteristic in respect with area PGa. E and F: The SMI-32 immuno-reactivity makes it possible to segment IPa from TE, (Lewis and Van Essen 2000) in area TE the SMI-32 immuno-reactive cells of layer 3 appear in highly aggregated multilayered clusters The limit between IPa and PGa is difficult to set in SMI-32 label. The limit between STP and PGa is quite clear as the labeled cells in layers 5 and 6 separate again in a bilaminar pattern and layer 3 is more densely labeled with large pyramids. Scale bars C and E: 1 mm, D and F: 0.5 mm.

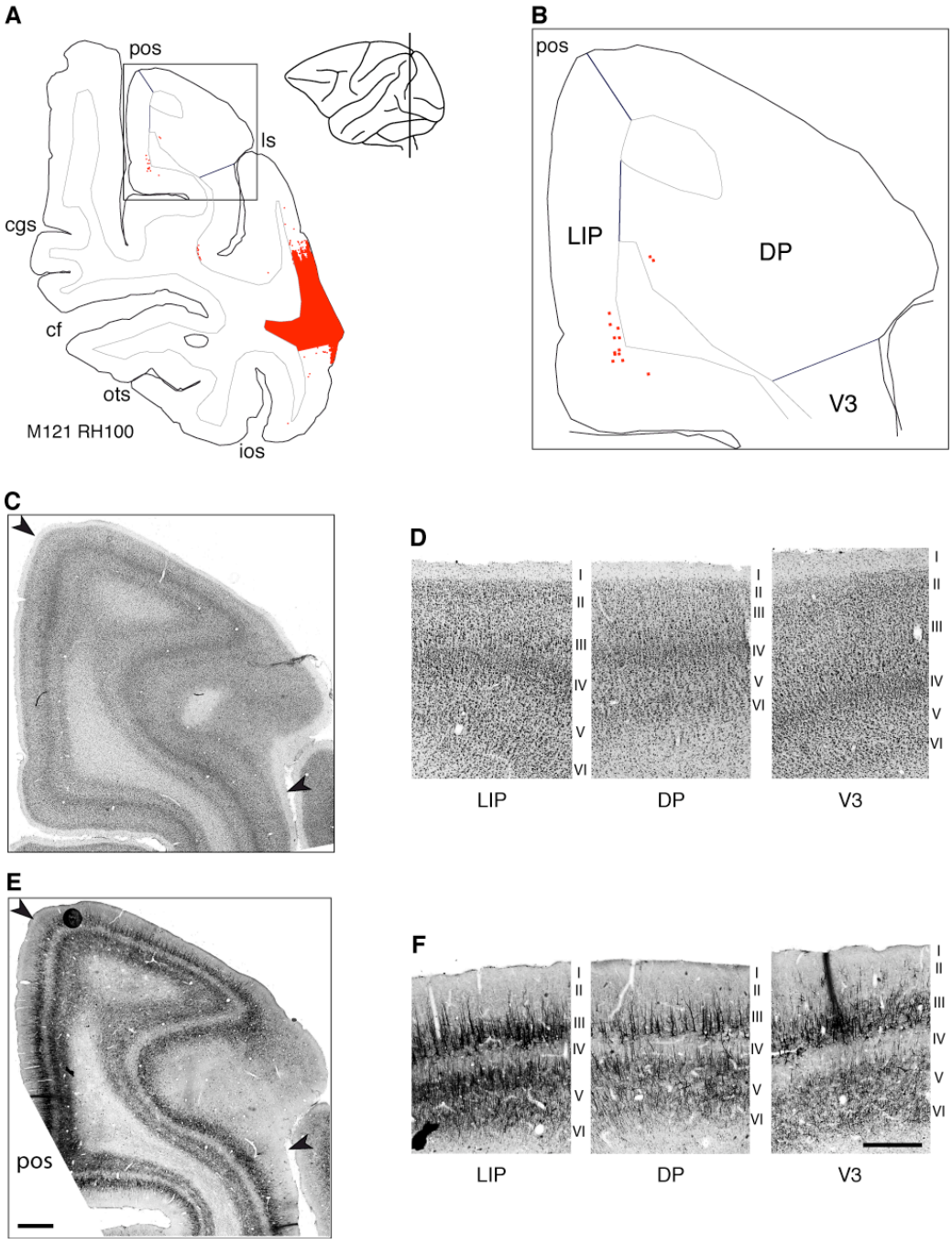

Fig S3. Illustration of the projection from DP onto area V1. A: Plot map of coronal section going across the injection site in area V1 and the projection zone in area DP. After stereotypic injections we consistently observe sparse labeling over many sections in area DP. B: Schematic drawing of a cortical hemisphere indicating the level of section and a zoom at the projection zone of DP. C and D: Low and high magnification photomicrographs of the section in A stained with the Nissl technique. High magnification shows the cytoarchitectonic of areas LIP, DP and V3. Area LIP has a well developed layer 4 and large pyramidal cells deep in layer 3 as well as in layer 5, layer 2 has a densely packed small cells. Also layer 3 shows a gradient in cell size with small cells at the level of limit with layer 2 and larger cells going more deeper, this makes it possible to differentiate between layers 2 and 3. In area DP layers 2 and 3 are less well distinguished. The global arrangement of cells is radial as in V4. The limit between DP and V3 is uncertain in Nissl stained sections. E and F: Low and high magnification photomicrographs of SMI-32 immuno-reactive at level corresponding to the section in A-D. Area LIP has very dense SMI-32 label with prominent layer 3 large pyramids having apical dendrites extending to the cortical surface. Layers 5 and 6 appear as two distinct laminar with darkly

stained neurites and cell bodies. Area DP presents less overall SMI-32 immuno-reactive and has a lighter stained layer 3 with large pyramidal cells having apical dendrites extending up to layer 2. Area DP has only rare stained cells in layer 2. This is a major difference with area V3, which has frequent small darkly stained pyramids in layer 2, which show short arborising apical dendrites. Layers 5 and 6 of area V3 is not distinguishable as two separate bands and are made largely of labeled neuropil in layer 6 and neuropil with stained cells in layer 5. (Hof and Morrison 1995). Scale bars C and E: 1 mm, D and F: 0.5 mm.

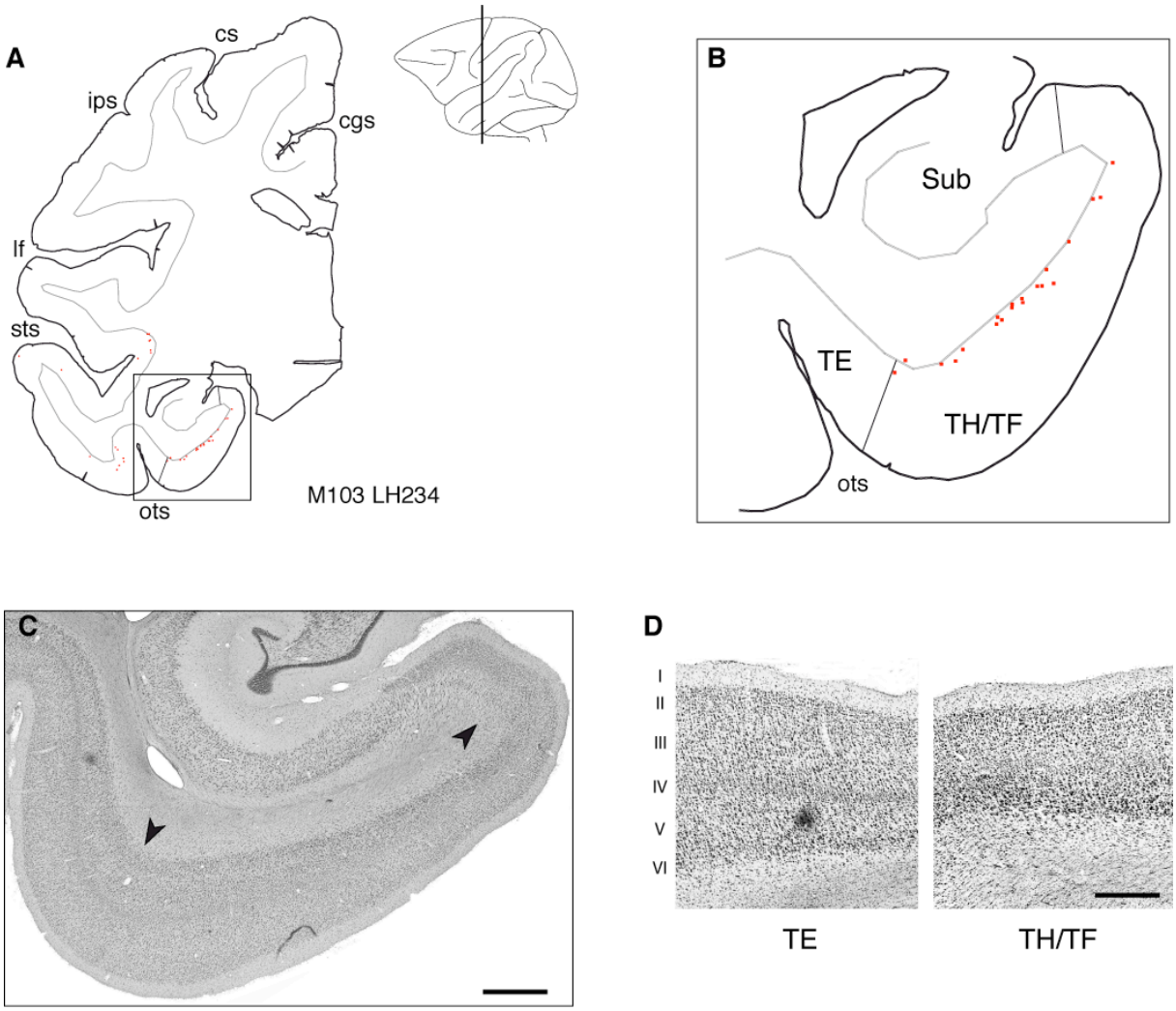

Fig S4. Illustration of The projection from the Parahippocampal complex (areas TH/TF) on to area V2. A: Injections in area V2 systematically generate labeling in areas TH/TF shown on a plot map of a coronal section. B: Zoom on the Parahipocampal cortex of the section in figure A and a lateral view of a hemisphere showing the level in section C. The cytoarchitectonic organization of the Parahippocampal cortex is well studied (Amaral et al, 2003). The parahippocampal cortex shows a gradient from agranular at anterio-medial levels of area TH to disgranular at the lateral limits of TF and caudal TH. The surrounding cortices have all a well-defined layer 4. This is the main criteria for the segmentation between TE and TF/TH. Layer 3 of TE is thicker with easier possibility to identify the sublayers 3A and 3B as well as the separation with layer 2. In TE the cells of layer 3 show an external-internal gradient of increasing size. There is a more clear-cut separation between layers 5 and 6 of TE than in TH/TF. Scale bars C: 1 mm, D: 0.5 mm

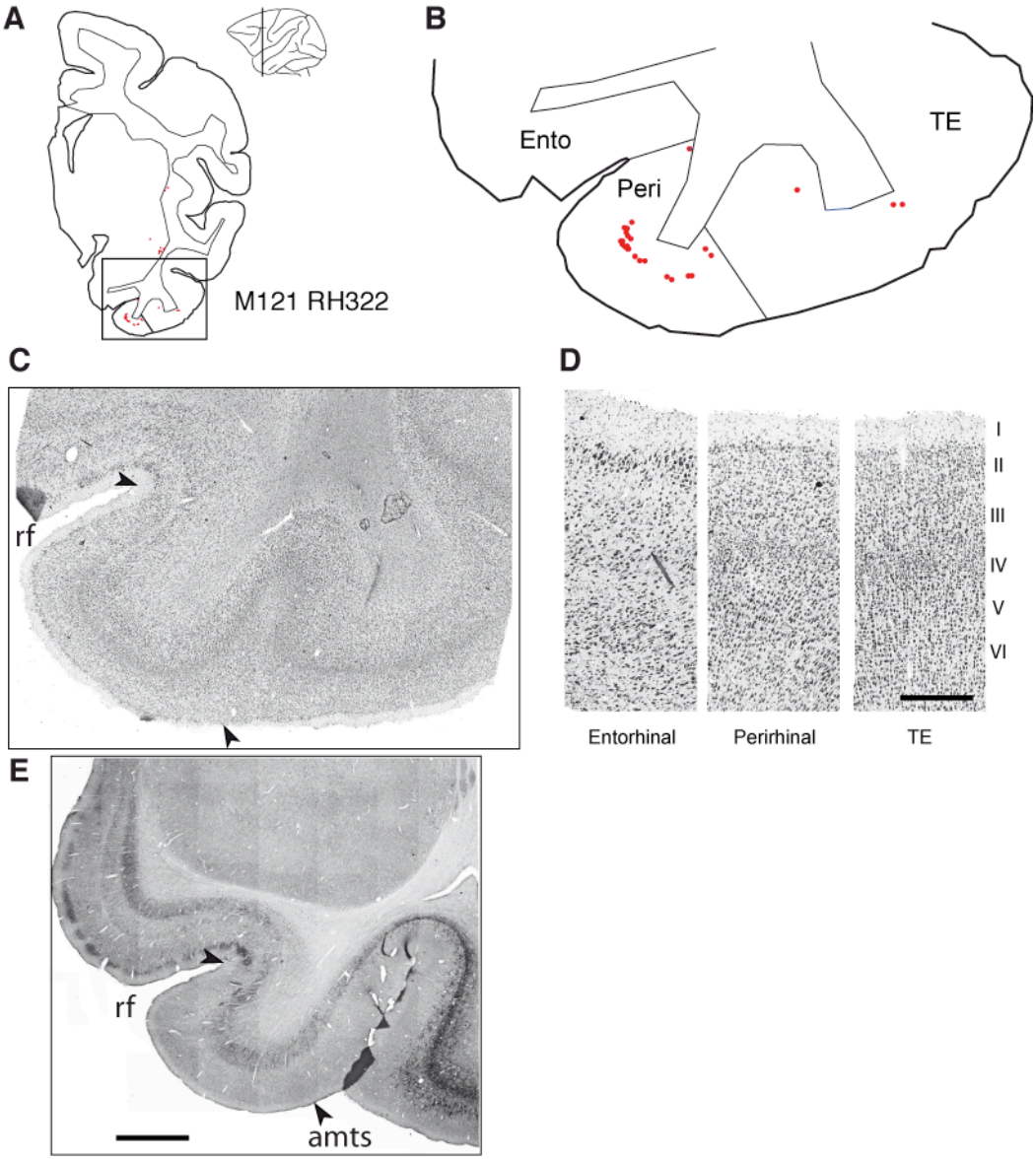

Fig S5: Projection from the perirhinal cortex on area V4 confirmed by histologic processing. **A** : Coronal section showing labeled cells following injection of fast blue into area V4. Section level is identified on brain hemisphere. **B**: Magnification of the section in **A** demonstrating the pattern of labeled cells projecting on V4. **C** : Low magnification of Nissl stain of the same section. **D**: Three photomicrographs showing cytoarchitectonic details of entorhinal cortex, perirhinal cortex and area TE. Entorhinal cortex is agranular with typical clusters of cells in layer II. Perirhinal cortex is disgranular with smaller clusters of 4-5 cells in layer II. Area TE is granular with completely developed layer IV and no aggregates in layer II. Layer III shows more radial arrangement of pyramids increasing their size with position depth. **E**: SMI-32 stained section at corresponding position. Entorhinal cortex is only weakly labeled with dark patches of neurites in layer II. Layers V and VI appear as separate bands of weakly labeled cells and neuropil. Perirhinal cortex shows very weakly stained cells and processes in layer V. Other layers are devoid of label. A gradient of darkly stained cells in layers III and V indicate the transition between perirhinal cortex and area TE (Amaral et al., 2003). Scale bars C and E: 1 mm, D: 0.5 mm

Figure S6: Atlas

Atlas

Index of abreviations

Areas

10	area 10
46d	area 46, dorsal part
46v	area 46, ventral part
11	area 11
12	area 12
14	area 14
9	area 9
32	area 32
9/46d	area 9/46, dorsal part
9/46v	area 9/46, ventral part
24c	area 24c
8B	area 8B
25	area 25
45	area 45
13	area 13
24b	area 24b
F6	frontal area F6
F7	frontal area F7
24a	area 24a
8	area 8
F2	frontal area F2
F3	frontal area F3
44	area 44
F5	frontal area F5
ProM	area ProM
OPAl	orbital periallocortex
OPRO	orbital proisocortex
Temporal pole	Temporal pole
Gu	gustatory cortex
Ins	insula
Pir	piriform
Peri	perirhinal
Ento	entorhinal
STPr	superior temporal polysensory, rostral part
TE	area TE
2/1	area 2/1
3	somatosensory area 3
IPa	area IPa
F4	fronta area F4
PGa	area PGa
S2	secondary somatosensory area
24d	area 24d

MB	medial belt
F1	frontal area F1
Core	core region of the auditory cortex
LB	lateral belt
PBr	parabelt, rostral part
1	somatosensory area 1
2	somatosensory area 2
23	area 23
29/30	area 29/30
Sub	subiculum
TH/TF	area TH/TF
STPi	superior temporal polysensory, intermediate part
2Ve	area 2, vestibular part
5	somatosensory area 5
7B	area 7B
AIP	anterior intraparietal area
PBc	parabelt, caudal part
VIP	ventral intraparietal area
LIP	lateral intraparietal area
FST	fundus of superior temporal area
TEO	area TEO
STPc	superior temporal polysensory, caudal part
V2	visual area 2
MIP	medial intraparietal area
31	area 31
MST	medial superior temporal area
PECg	parietal area PE, cingulate part
V3	visual area 3
V4	visual area 4
Prost	prostriata
7A	area 7A
MT	middle temporal area
TPt	temporo-parietal area
V4t	transitional visual area 4
Pgm	parietal area Pg, medial part
V1	visual area 1
PIP	posterior intraparietal area
V3A	visual area 3A
DP	dorsal prelunate area
PO	parieto-occipital area

Sulci

ps	principal sulcus
morb	medial orbital sulcus
ros	rostral sulcus
cis	cingulate sulcus
lorb	lateral orbital sulcus
asu	arcuate sulcus upper limb
asl	arcuate sulcus lower limb
lf	lateral fissure
sts	superior temporal sulcus
rf	rhinal fissure
amts	anterior middle temporal sulcus
sas	spur of the arcuate sulcus
cs	central sulcus
ots	occipito-temporal sulcus
ips	intraparietal sulcus
pmts	posterior middle temporal sulcus
cas	calcarine sulcus
ios	inferior occipital sulcus
lus	lunate sulcus
col	collateral sulcus
pos	parieto-occipital slucus

p. 01

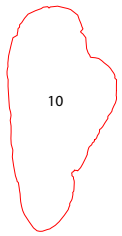

4000 µm

p. 02

4000 µm

p. 03

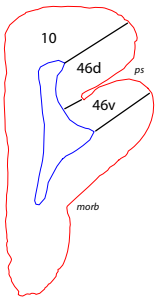

4000 µm

p. 04

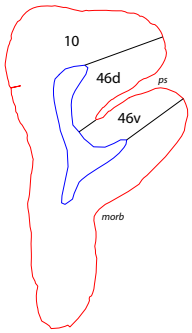

4000 µm

p. 05

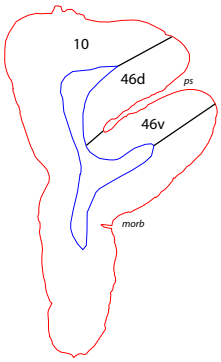

4000 µm

p. 06

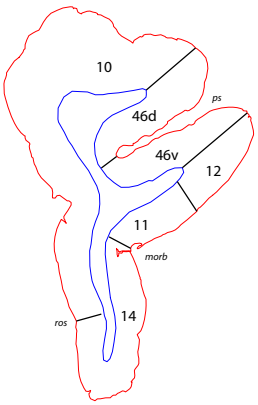

4000 µm

p. 07

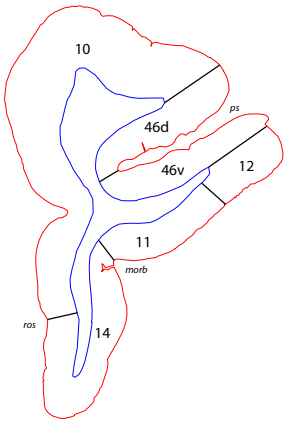

4000 µm

p. 08

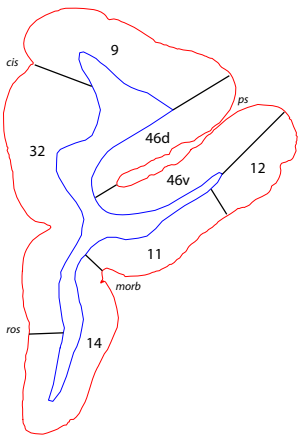

4000 µm

p. 09

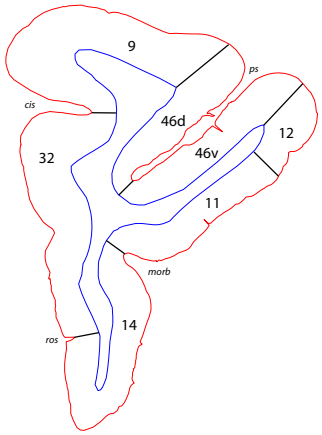

4000 µm

p. 10

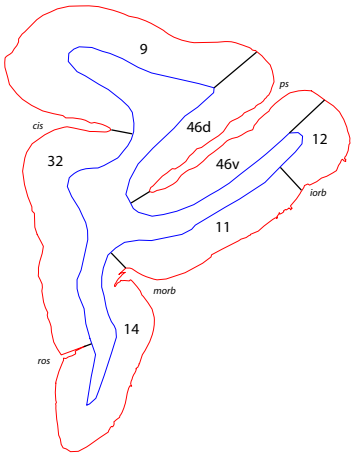

4000 µm

p. 11

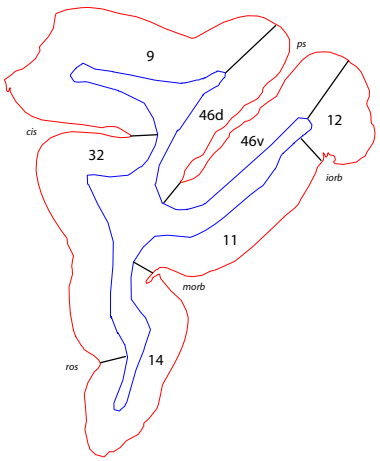

4000 µm

p. 12

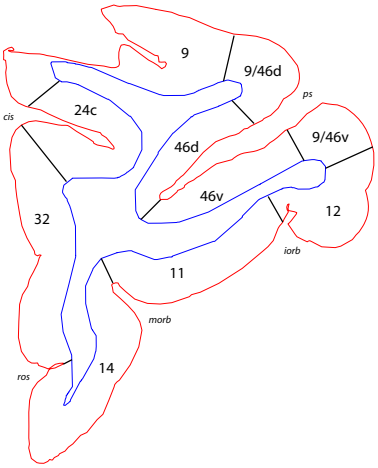

4000 µm

p. 13

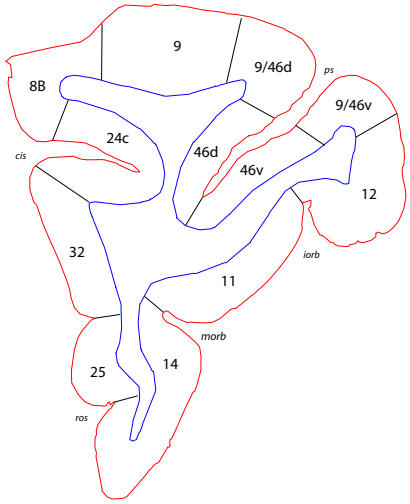

4000 µm

p. 14

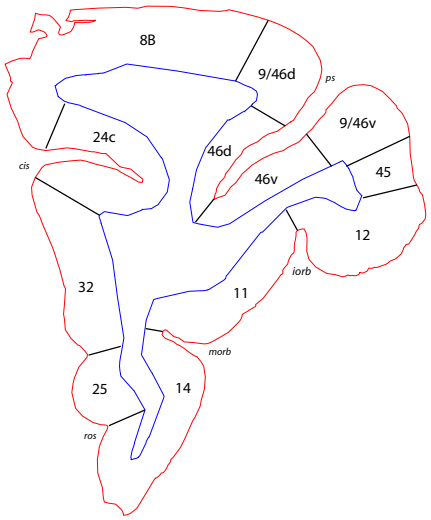

4000 µm

p. 15

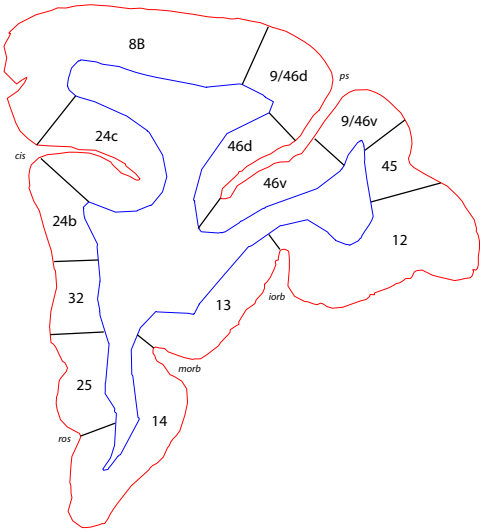

4000 µm

p. 16

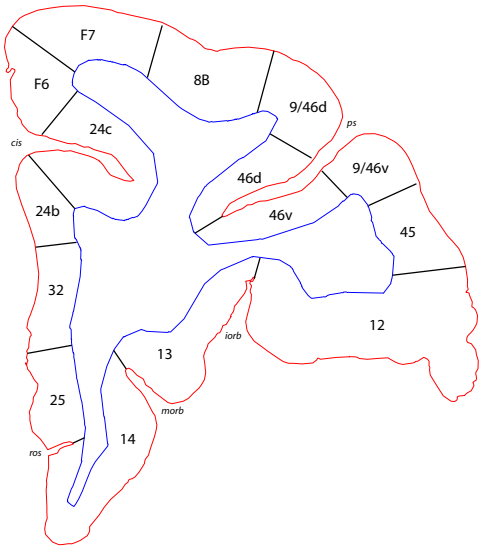

4000 µm

p. 17

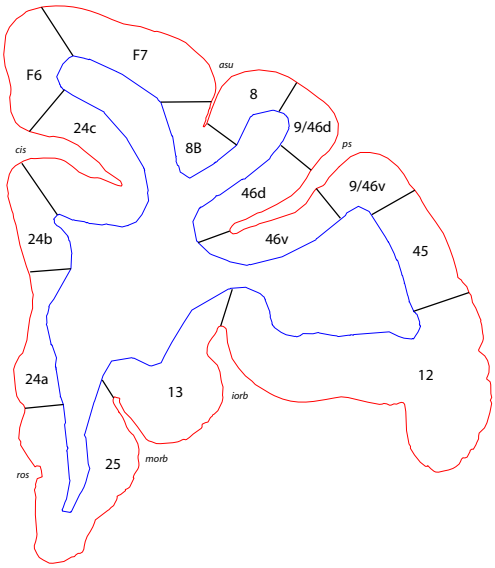

4000 µm

p. 18

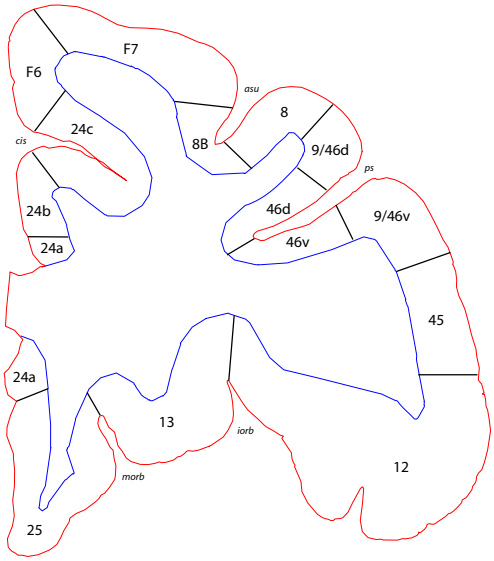

4000 µm

p. 19

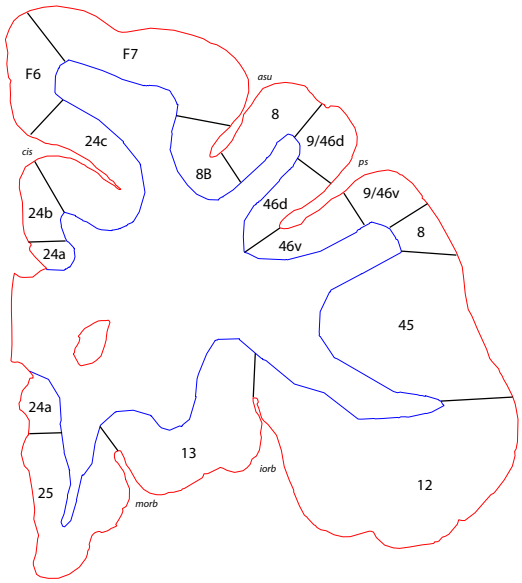

4000 µm

p. 20

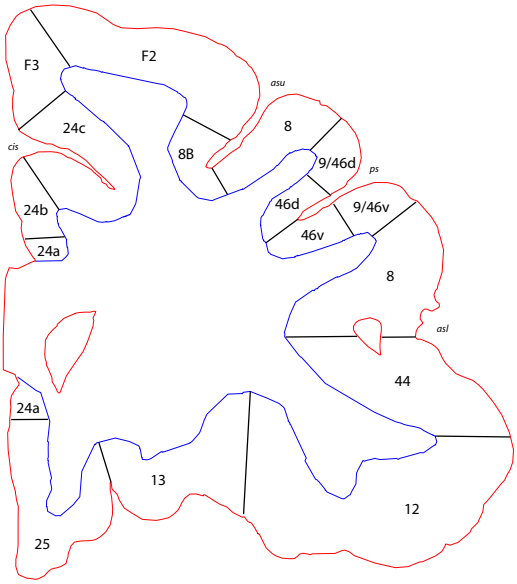

4000 µm

p. 21

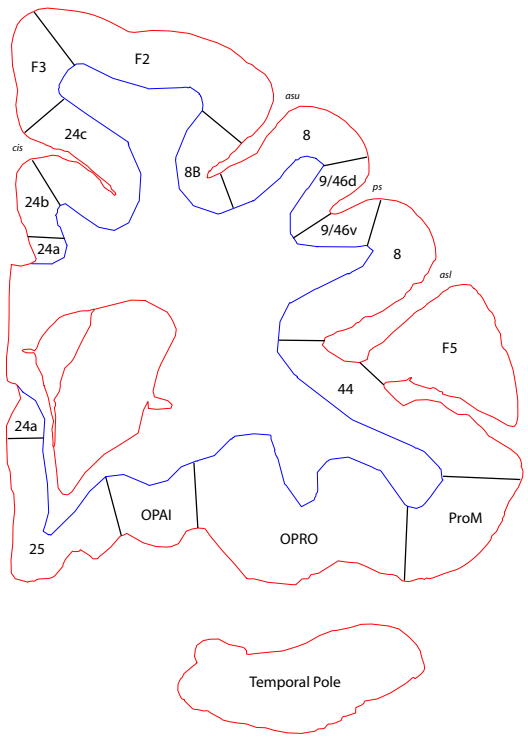

4000 µm

p. 22

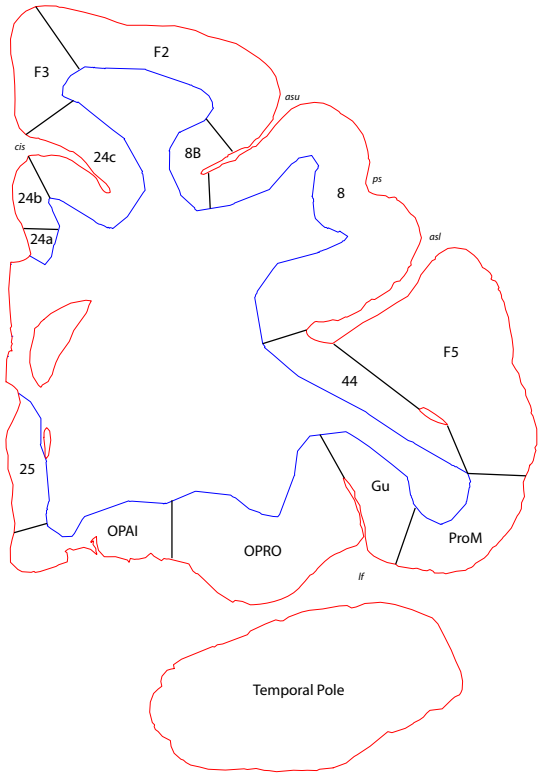

4000 µm

p. 23

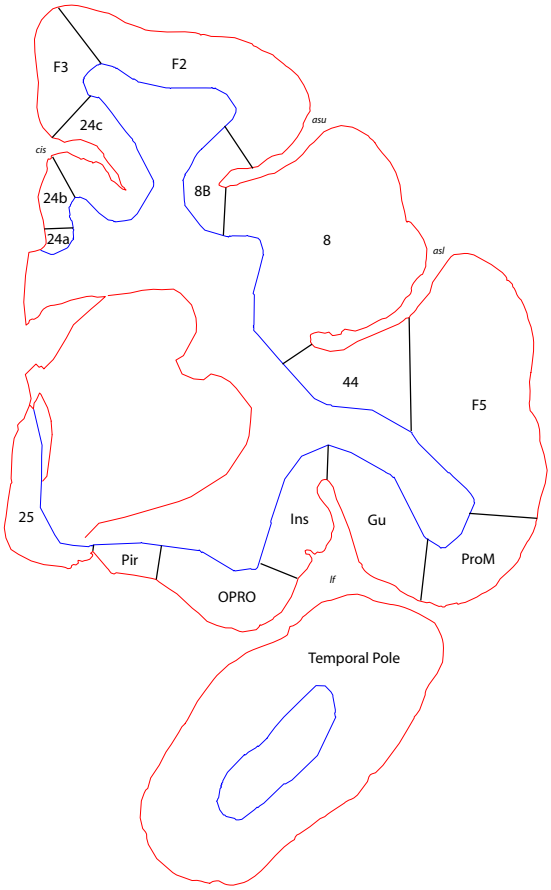

4000 µm

p. 24

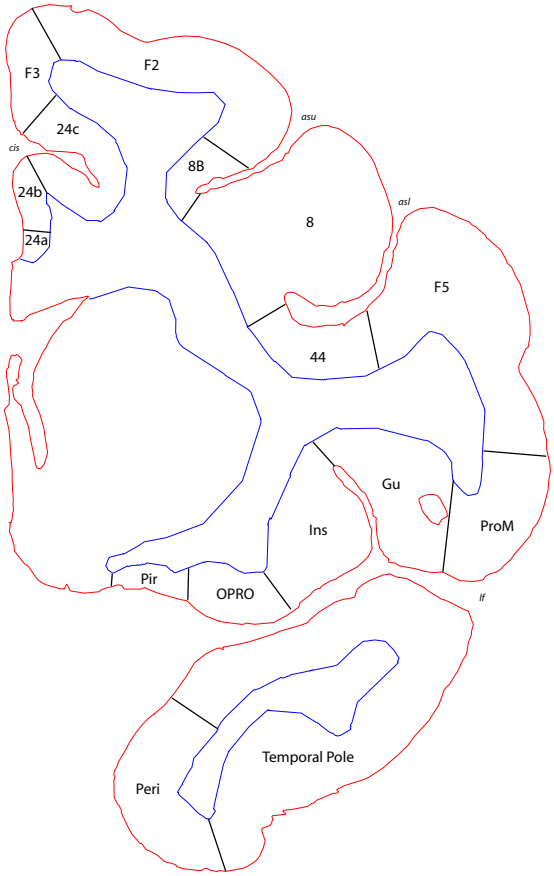

4000 µm

p. 25

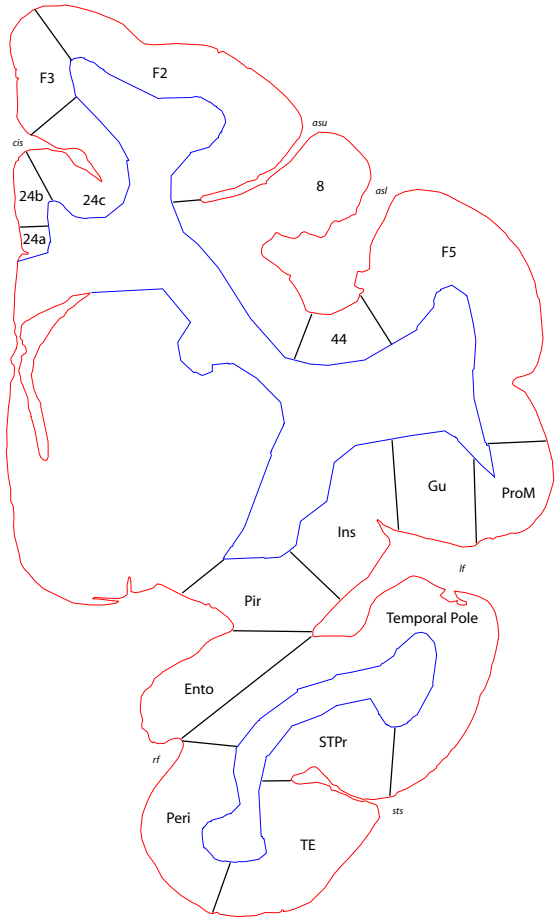

4000 µm

p. 26

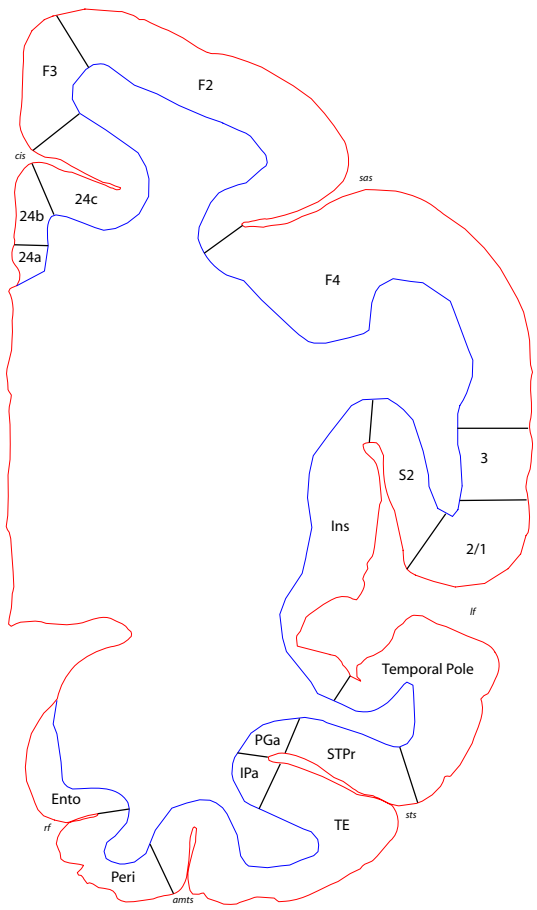

4000 µm

p. 27

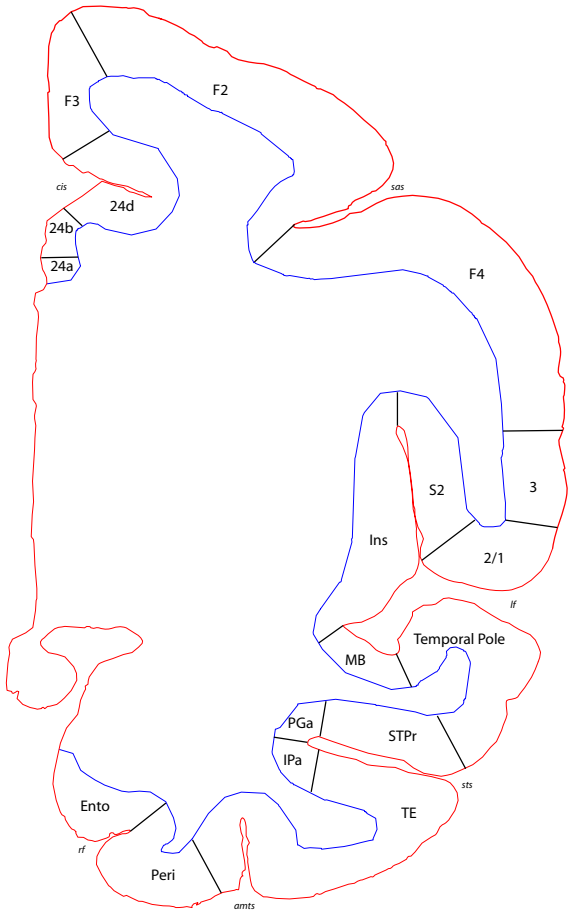

4000 µm

p. 28

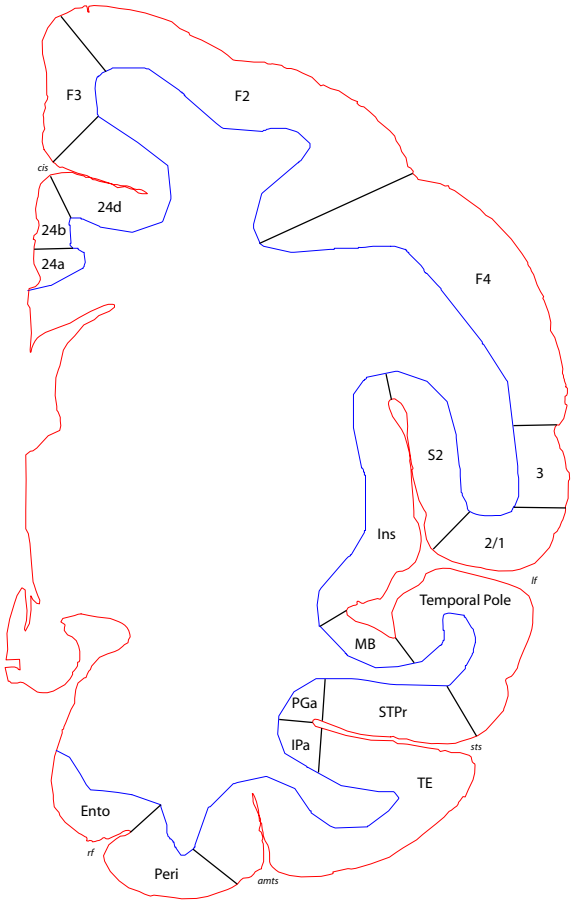

4000 µm

p. 29

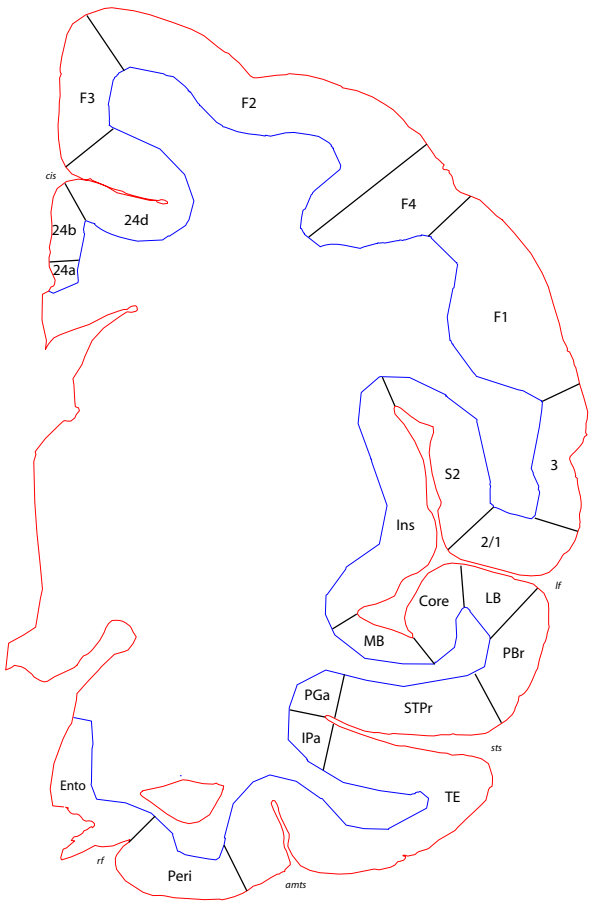

4000 µm

p. 30

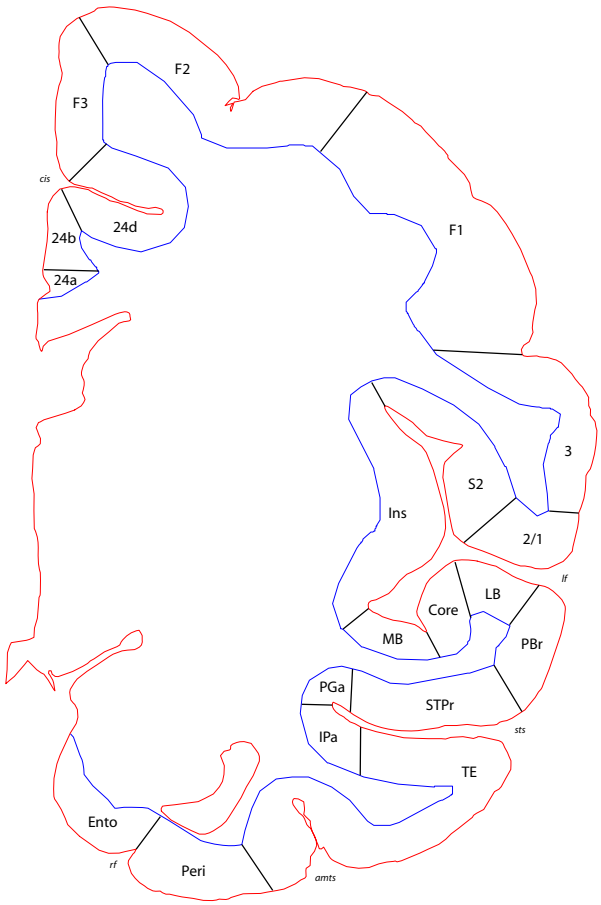

4000 µm

p. 31

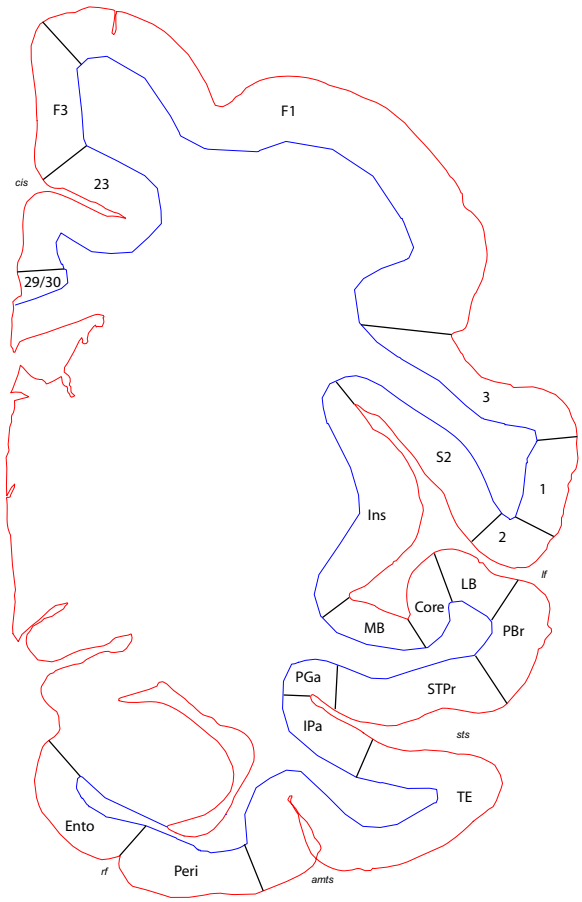

4000 µm

p. 32

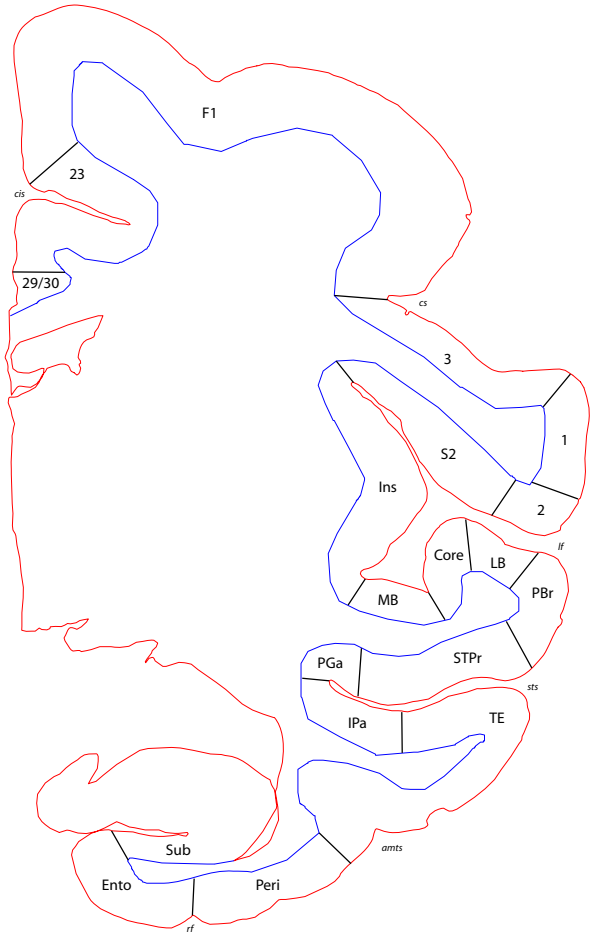

4000 µm

p. 33

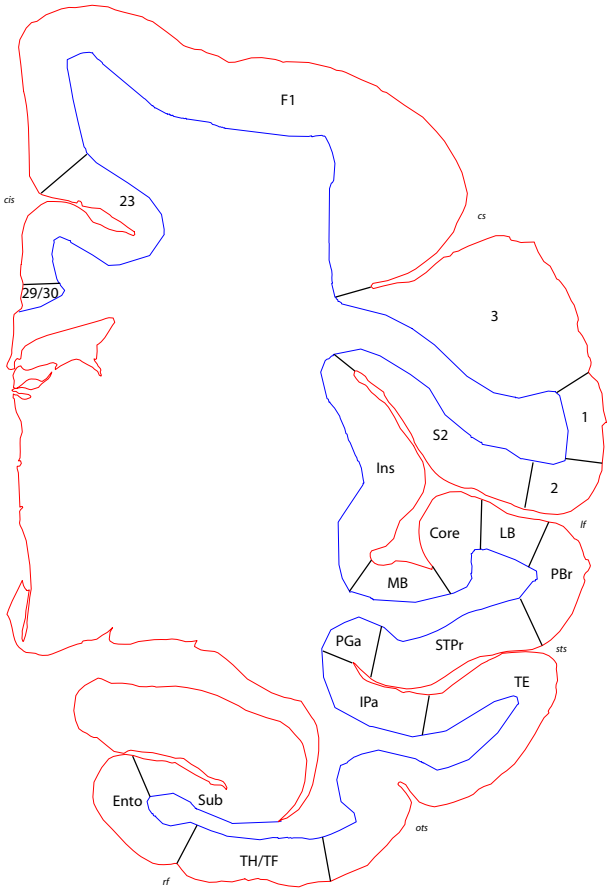

4000 µm

p. 34

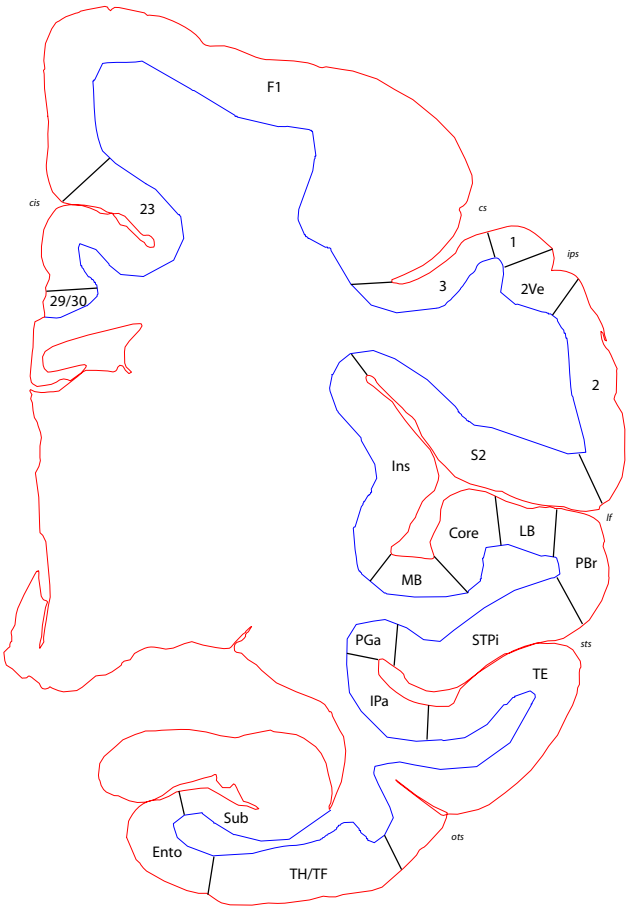

4000 µm

p. 35

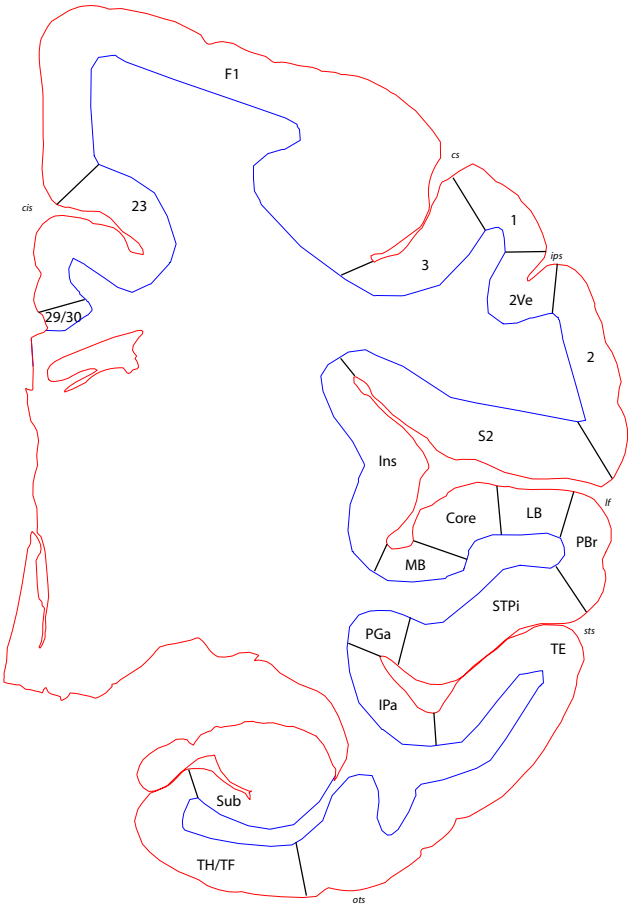

4000 µm

p. 36

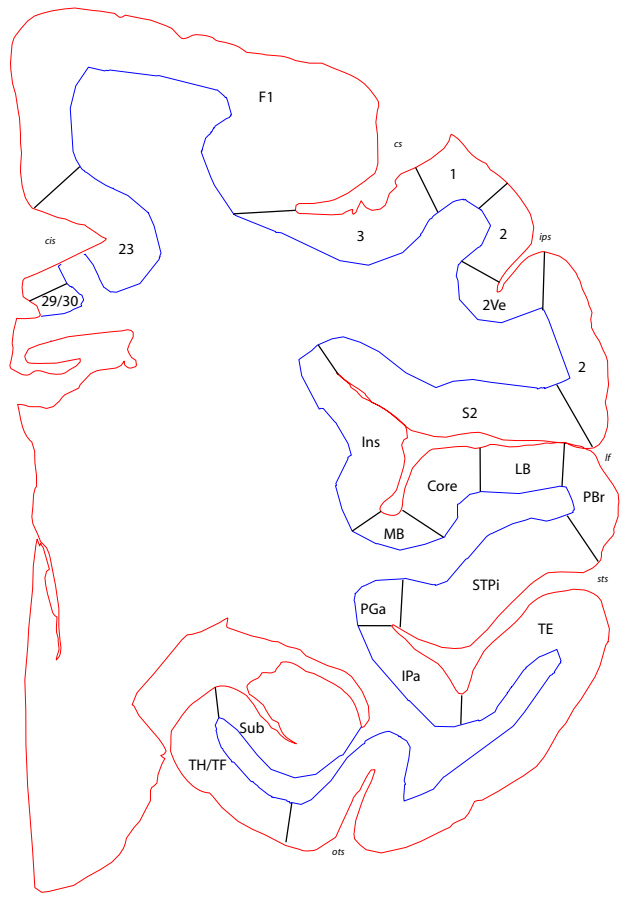

4000 µm

p. 37

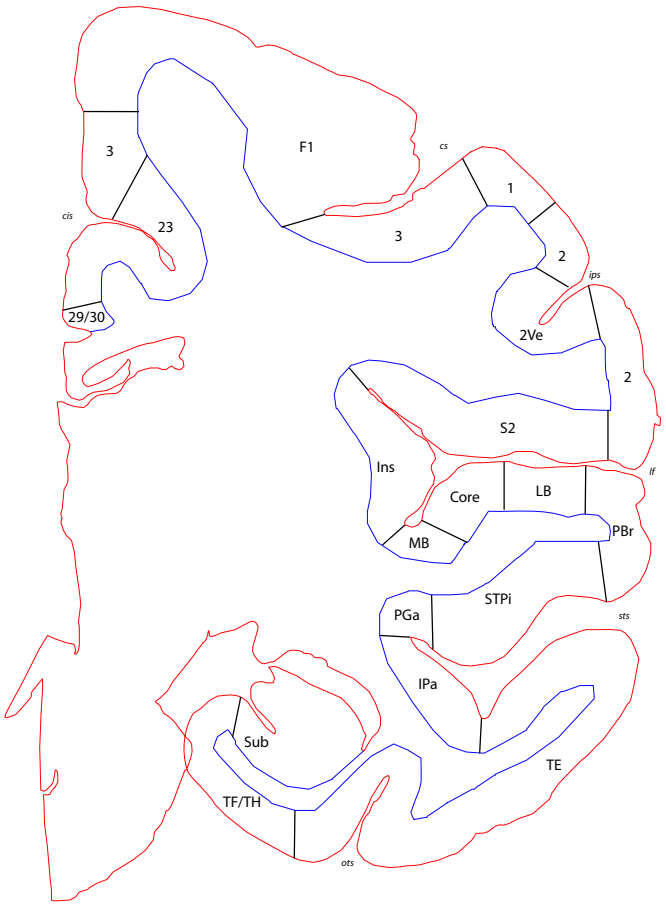

4000 µm

p. 38

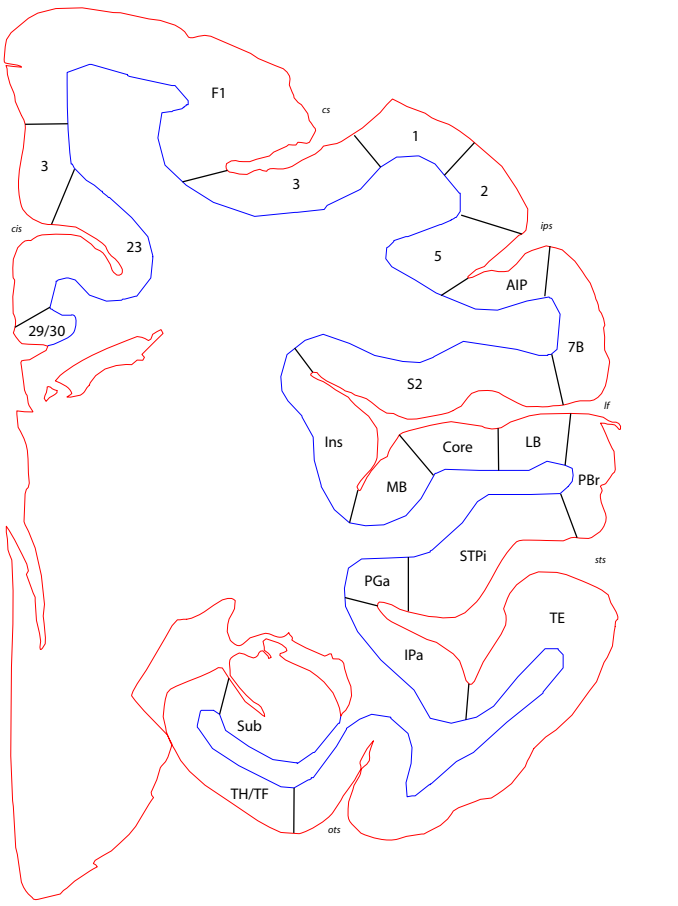

4000 µm

p. 39

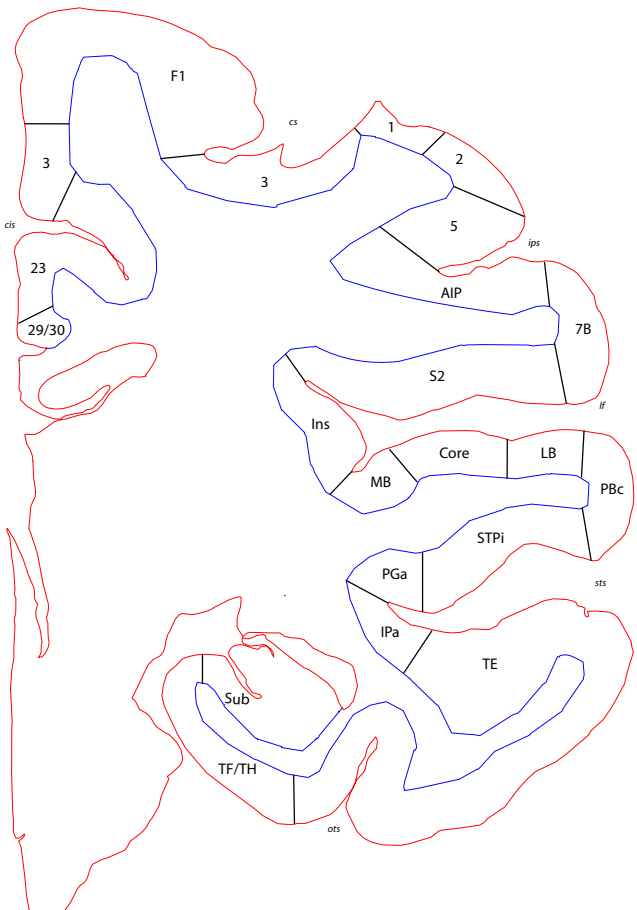

4000 µm

p. 40

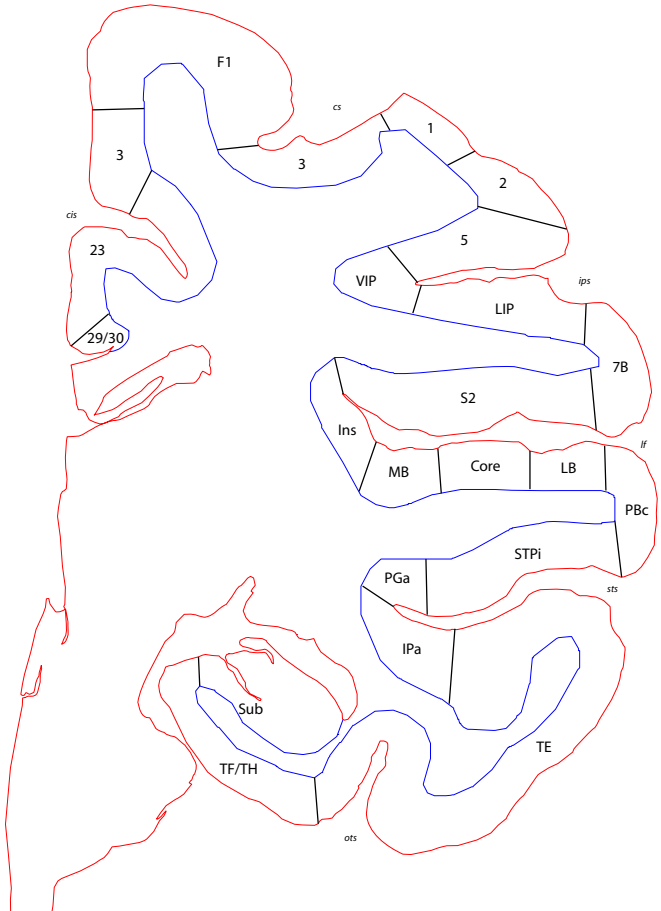

4000 µm

p. 41

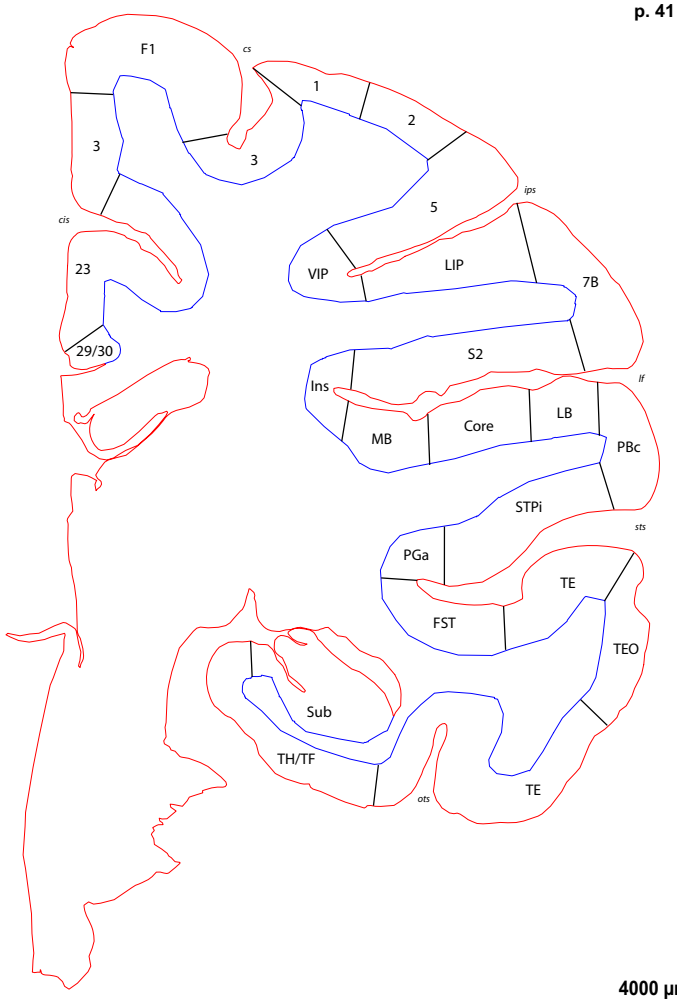

4000 µm

p. 42

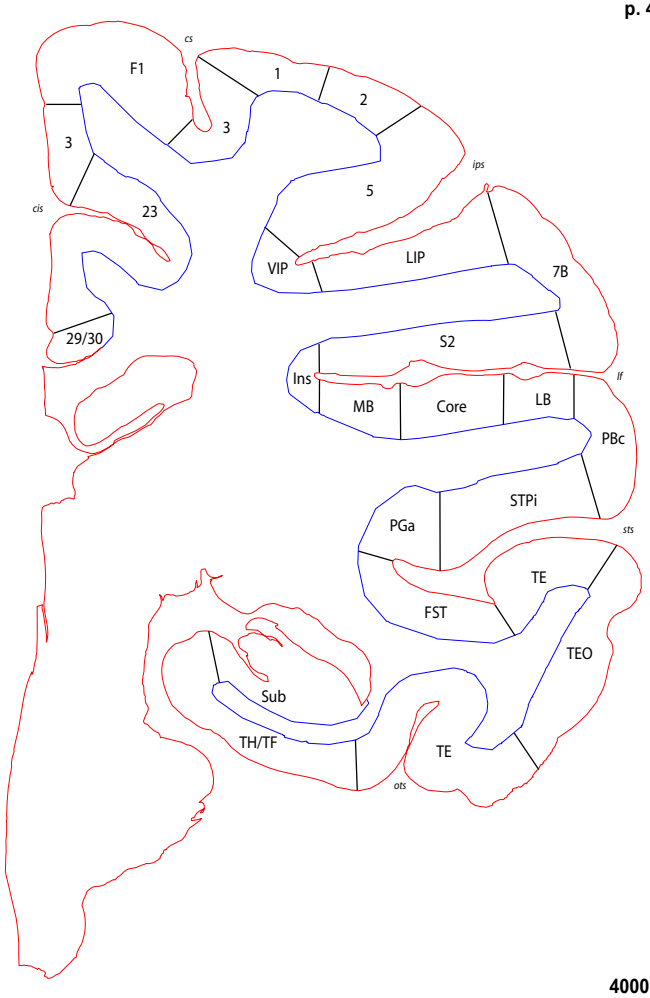

4000 µm

p. 43

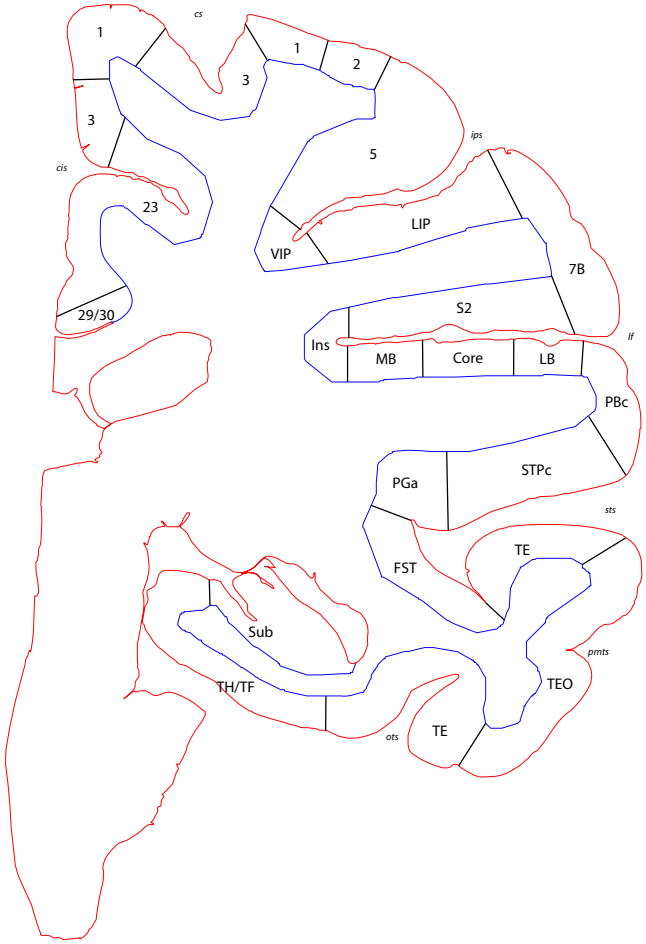

4000 µm

p. 44

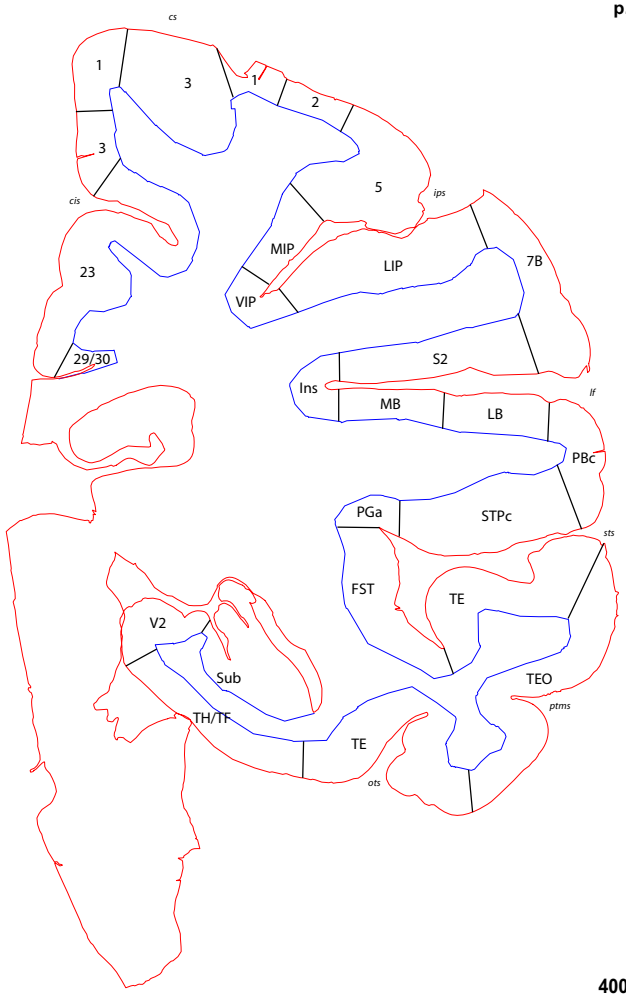

4000 µm

p. 45

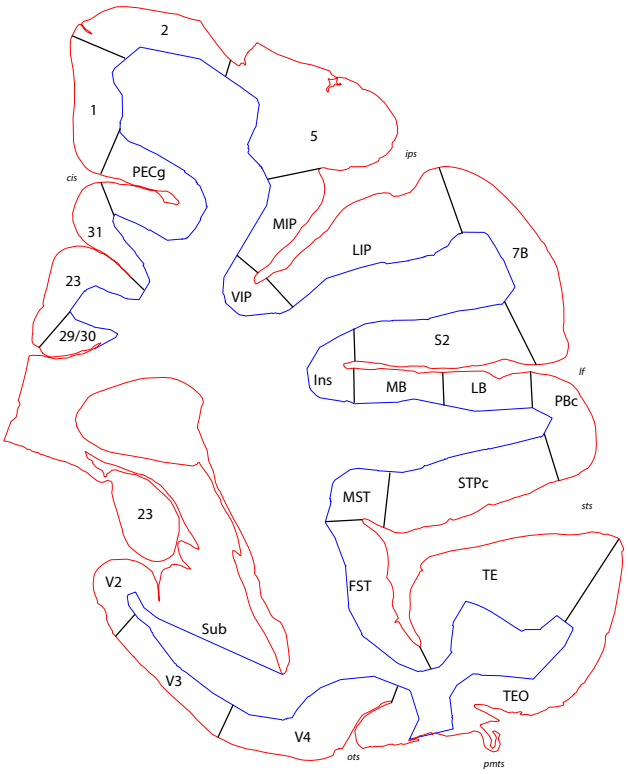

4000 µm

p. 46

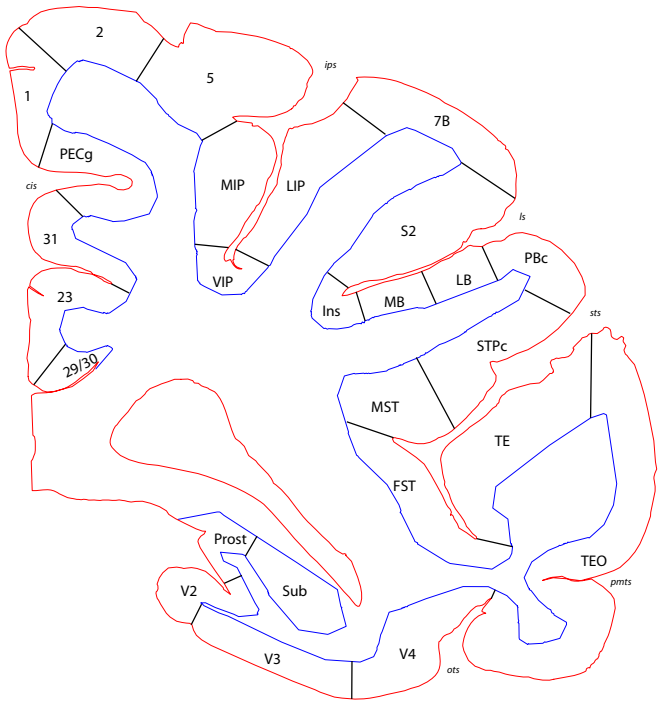

4000 µm

p. 47

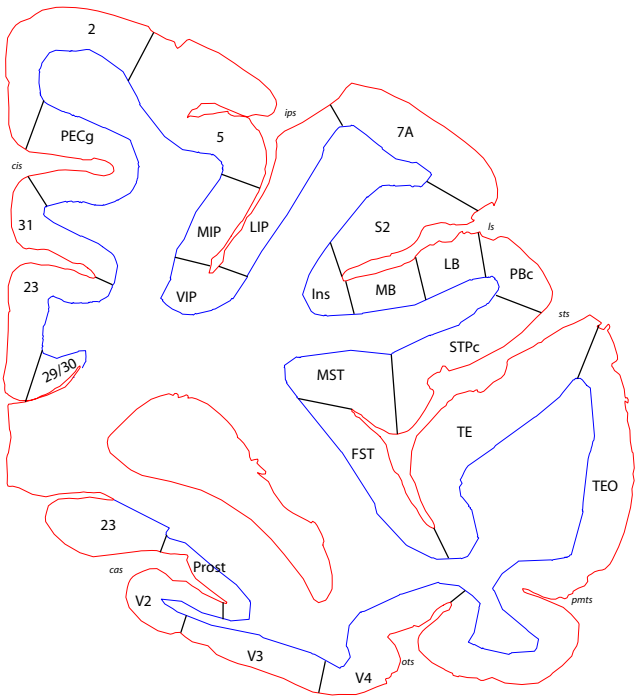

4000 µm

p. 48

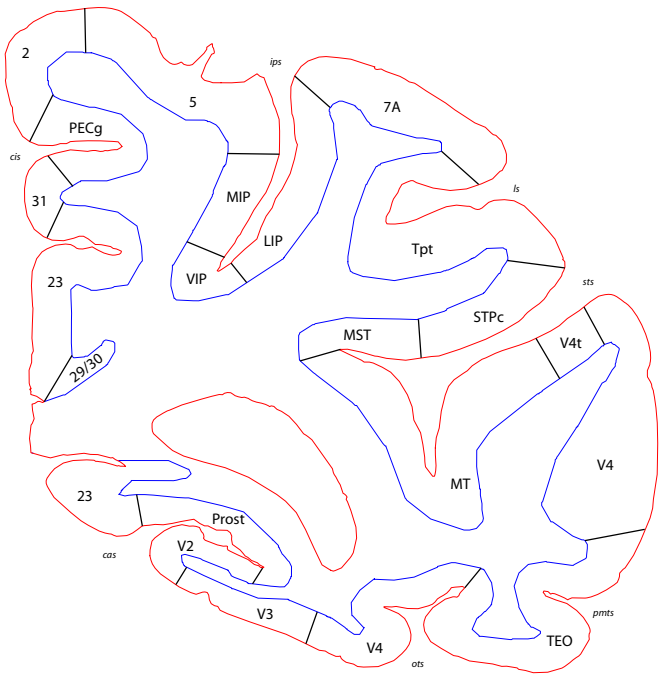

4000 µm

p. 49

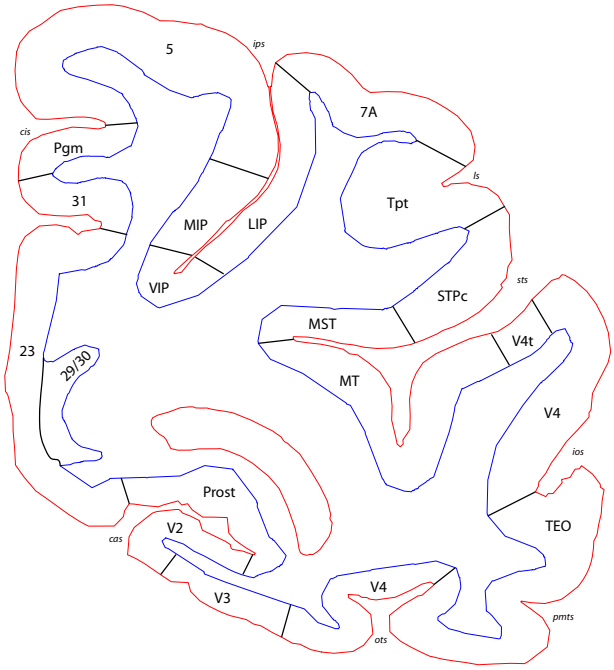

4000 µm

p. 50

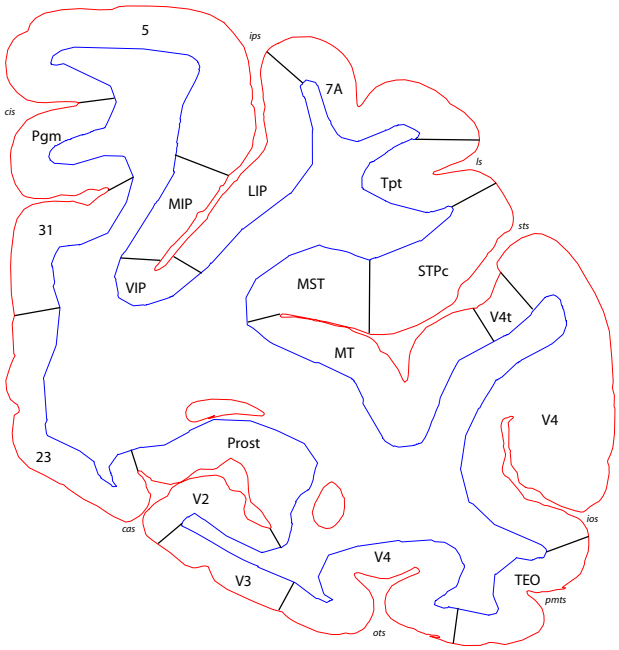

4000 µm

p. 51

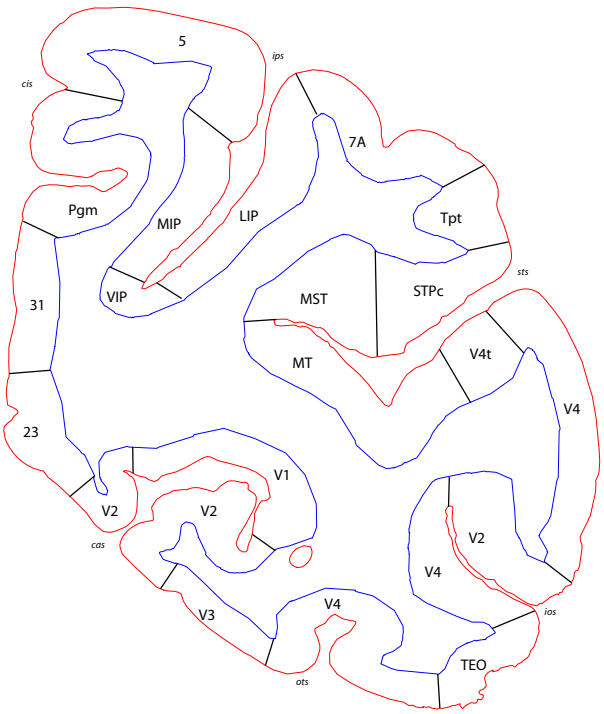

4000 µm

p. 52

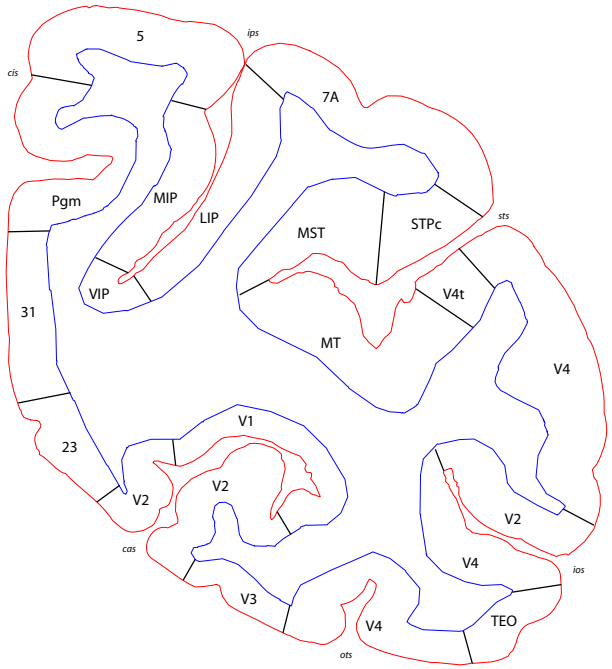

4000 µm

p. 53

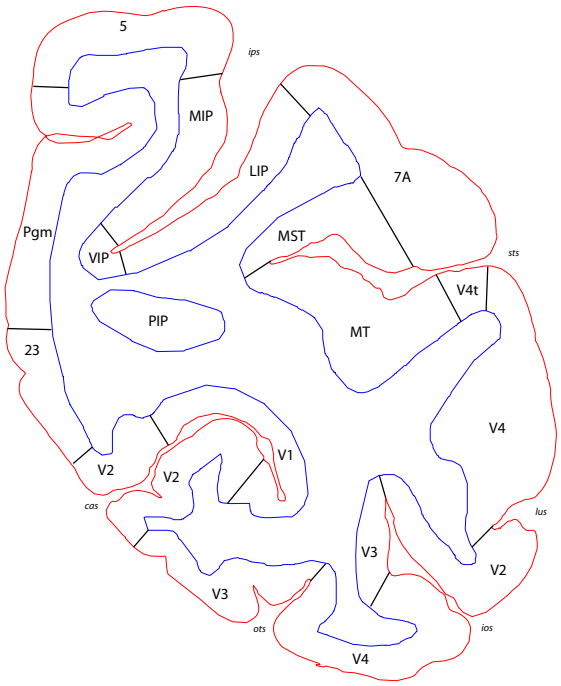

4000 µm

p. 54

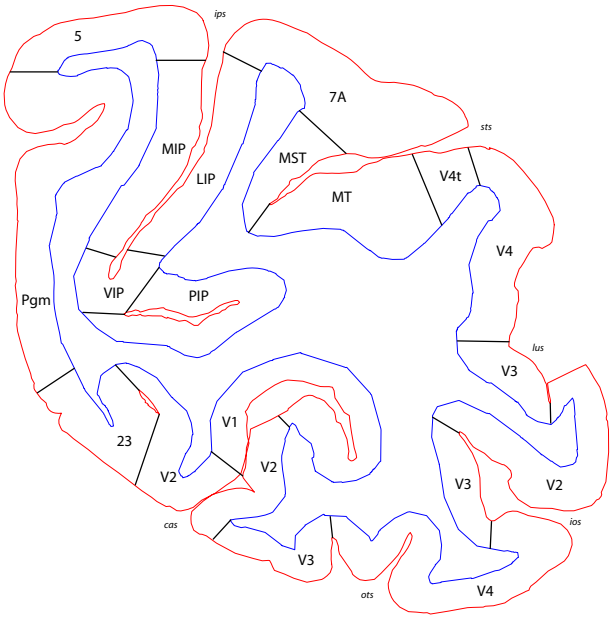

4000 µm

p. 55

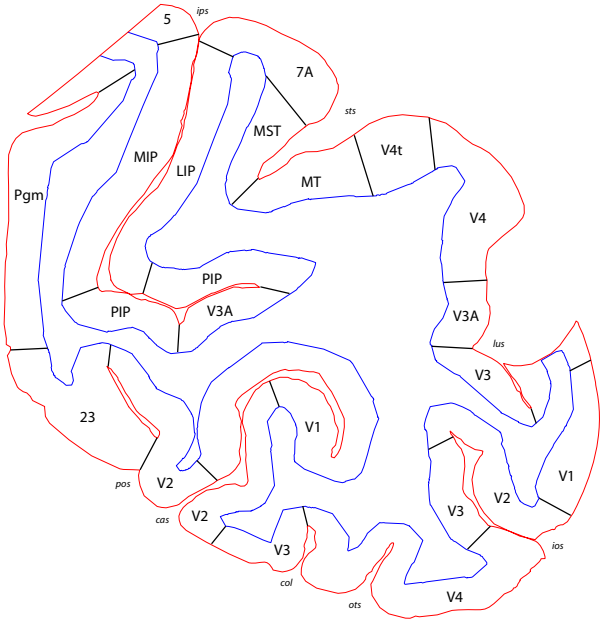

4000 µm

p. 56

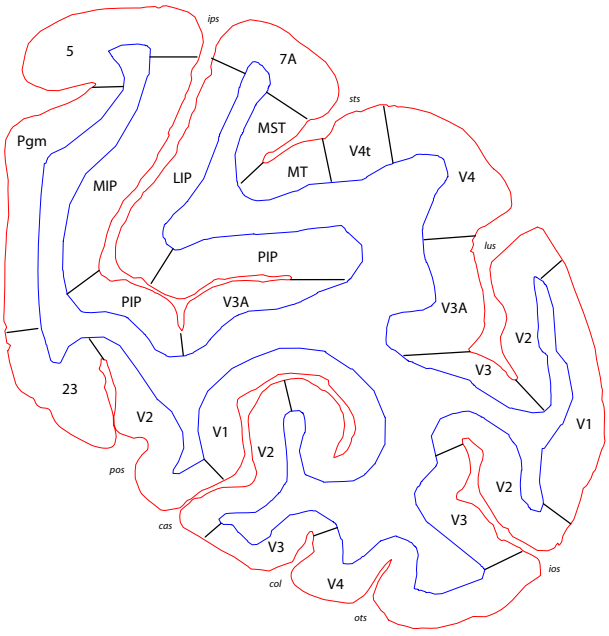

4000 µm

p. 57

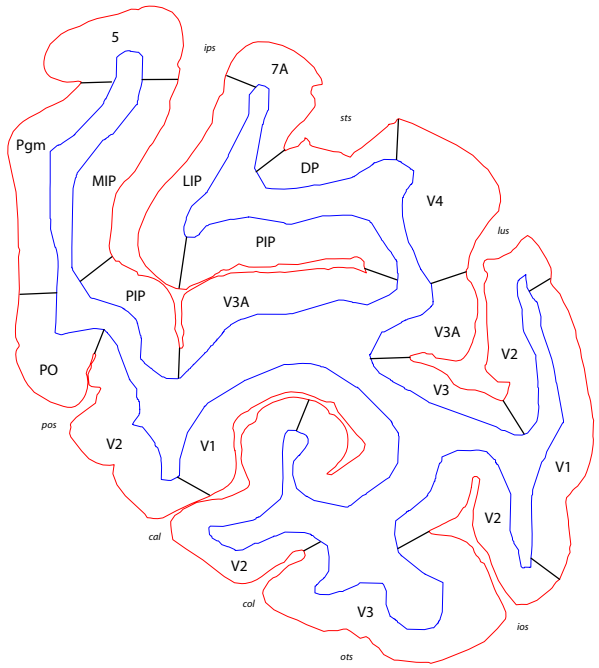

4000 µm

p. 58

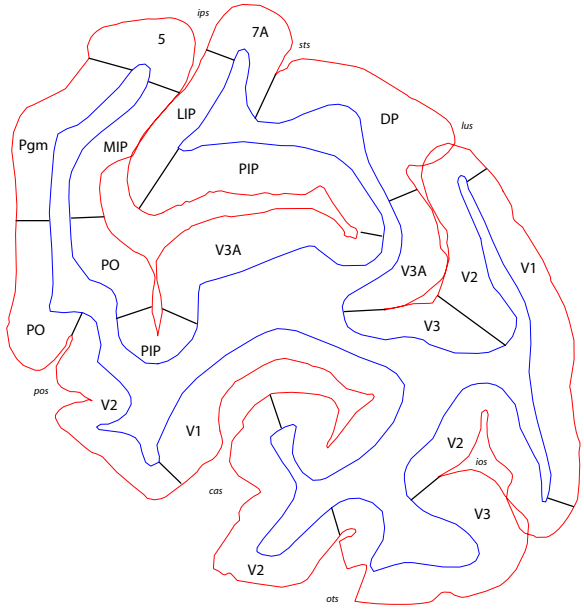

4000 µm

p. 59

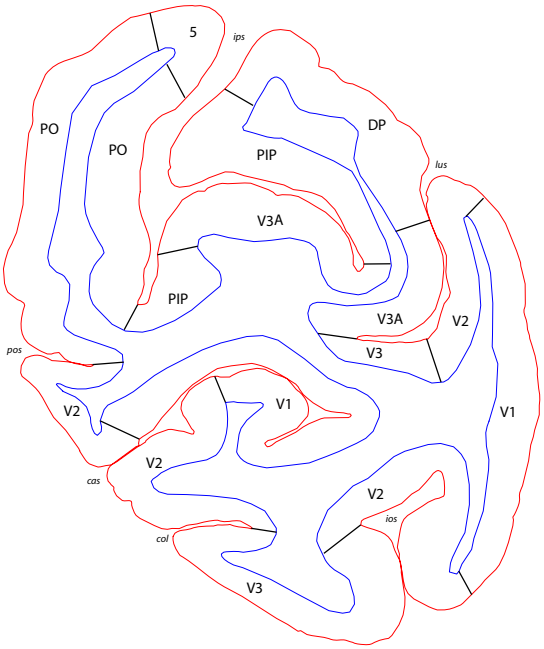

4000 µm

p. 60

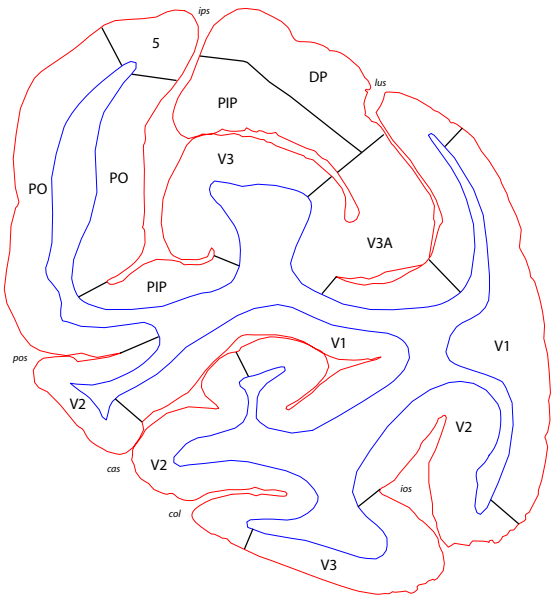

4000 µm

p. 61

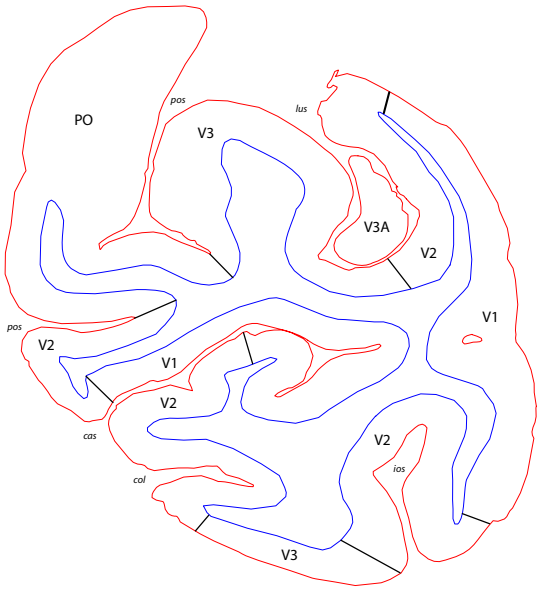

4000 µm

p. 62

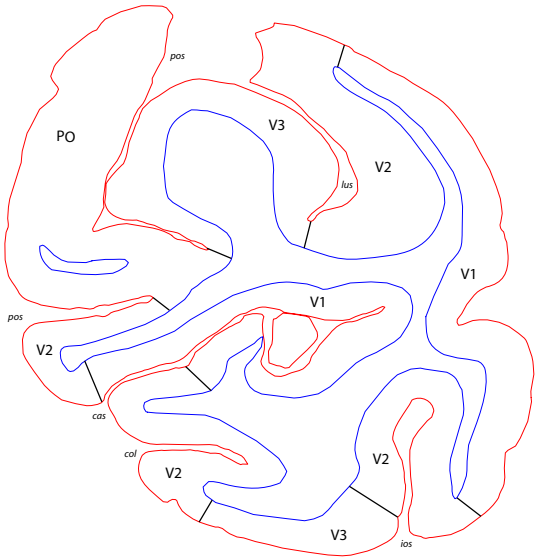

4000 µm

p. 63

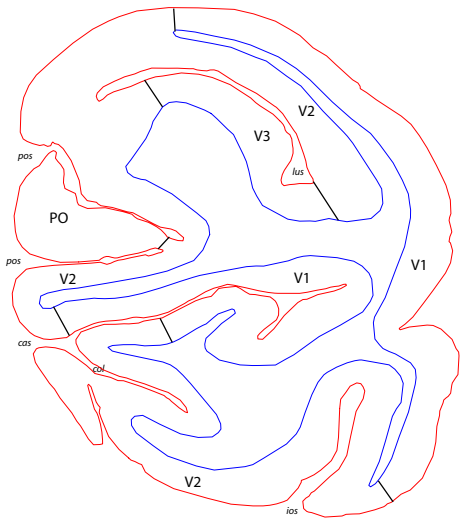

4000 µm

p. 64

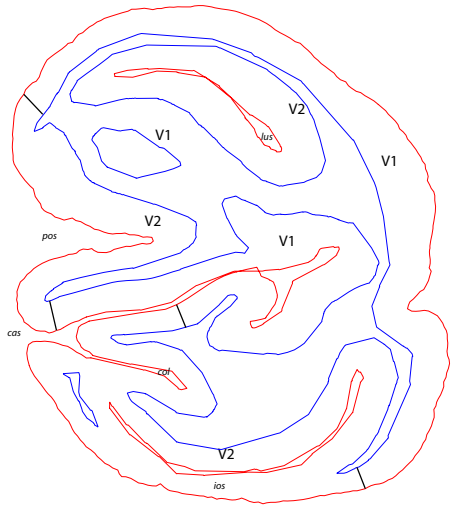

4000 µm

p. 65

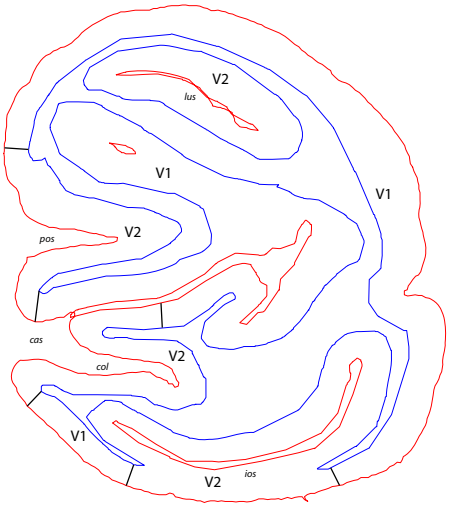

4000 µm

p. 66

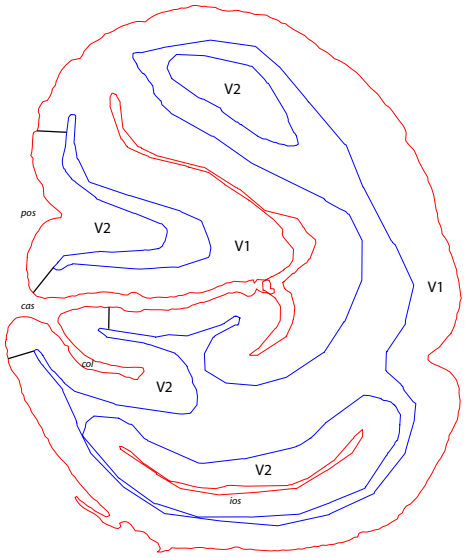

4000 µm

p. 67

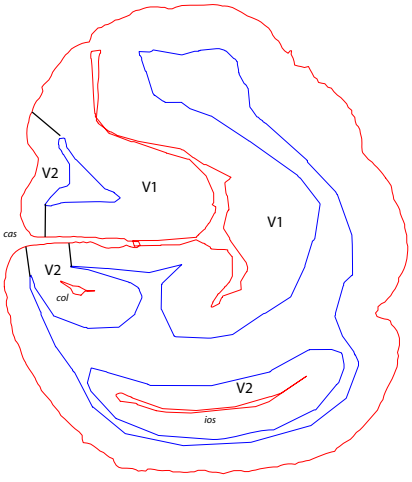

4000 µm

p. 68

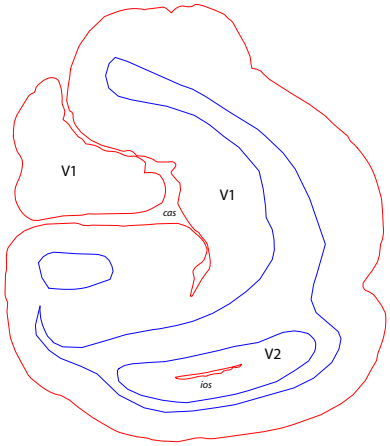

4000 µm

p. 69

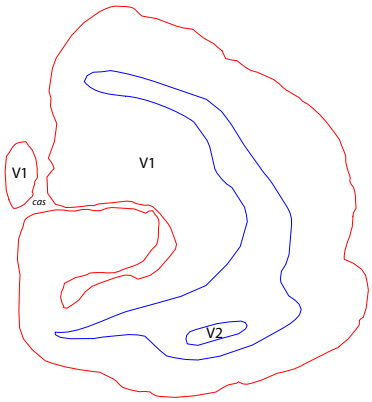

4000 µm

p. 70

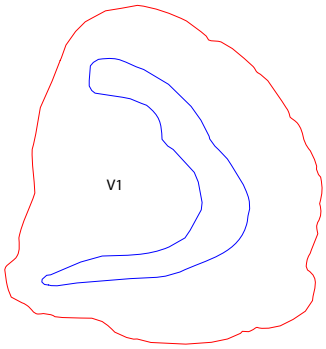

4000 µm

p. 71

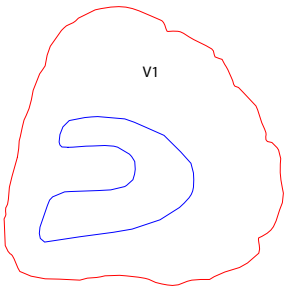

4000 µm

p. 72

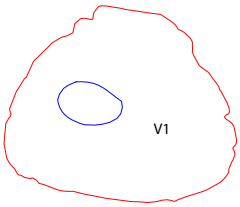

4000 µm

4000 µm

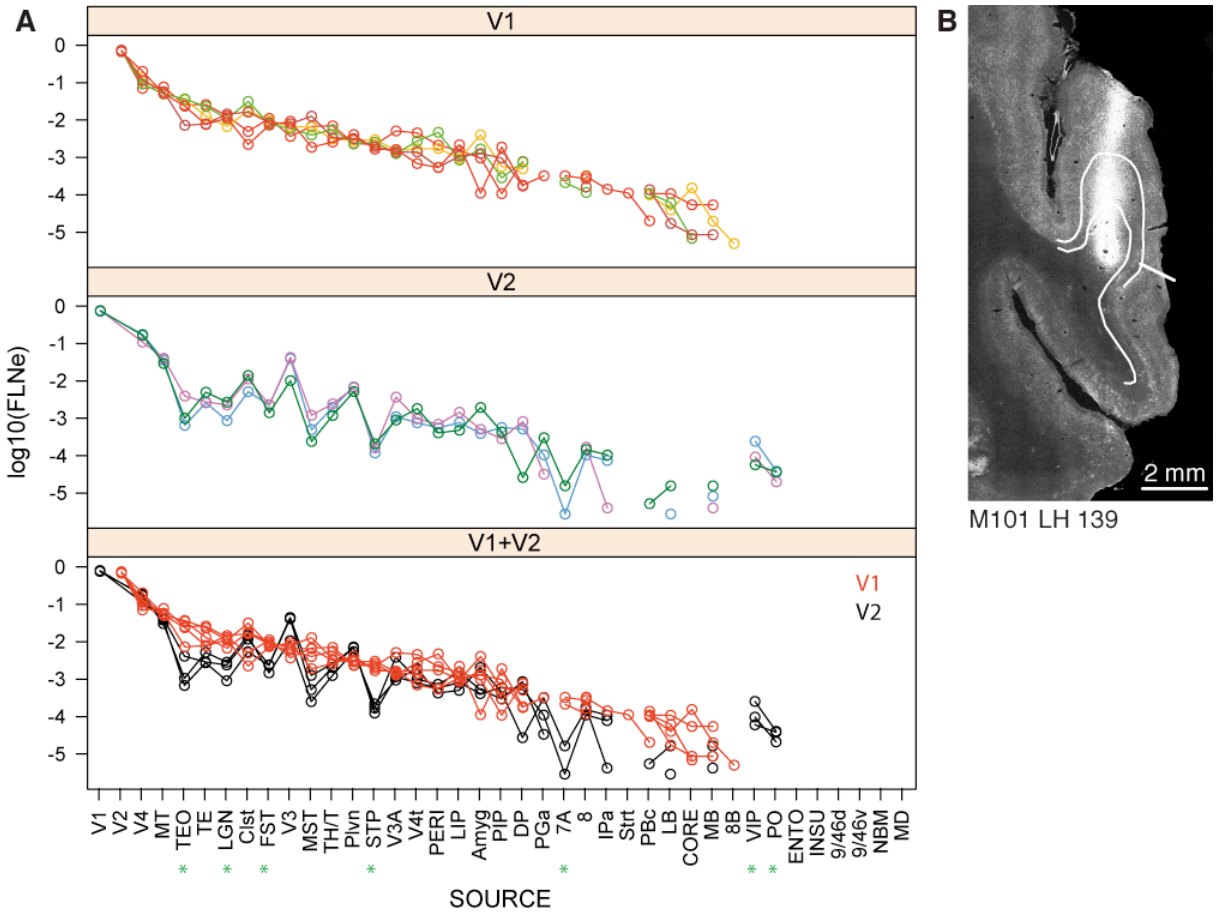

Figure S7: FLN distribution for V1 and V2 showing the M101 LH is characteristic of V2 and not V1.

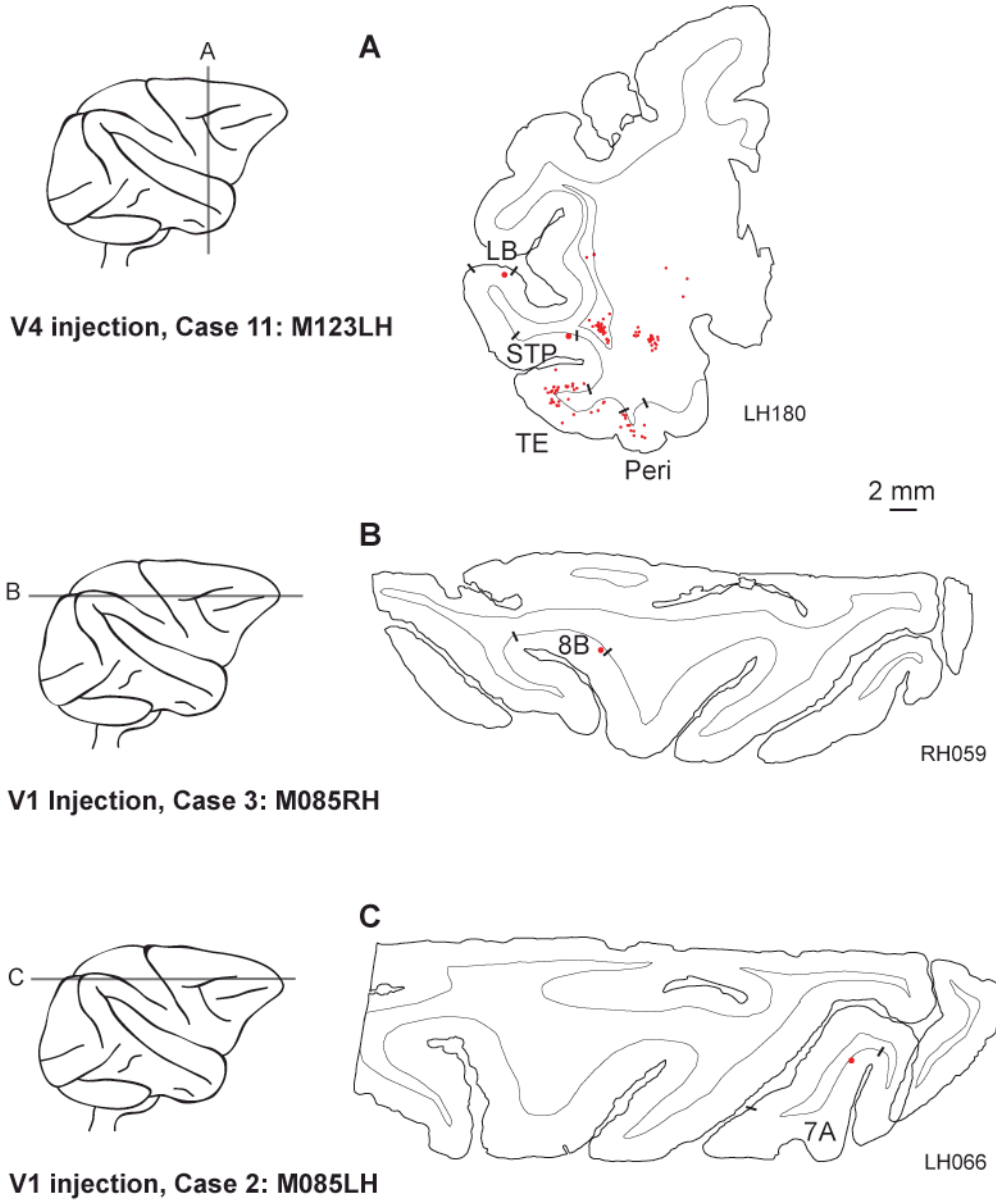

Figure S8: Projection zones A) Injection V4 projection from LB; B) Injection V1 projection from 8B; C) Injection V1 projection from 7A;

Supplementary references

Amaral DG, Behniea H, Kelly JL. 2003. Topographic organization of projections from the amygdala to the visual cortex in the macaque monkey. Neuroscience. 118: 1099-1120.

Barone P, Dehay C, Berland M, Bullier J, Kennedy H. 1995. Developmental remodeling of primate visual cortical pathways. Cereb Cortex. 5: 22-38.

Kennedy H, Bullier J, Dehay C. 1989. Transient projection from the superior temporal sulcus to area 17 in the newborn macaque monkey. Proc Natl Acad Sci U S A. 86: 8093-8097.

Kuypers HGJM, Bentivoglio M, Catsman-Berrevoets CE, Bahros AT. 1980. Double retrograde neuronal labelling through divergent axon collaterals using two fluorescent tracers with the same ecitation wave length which label different features of the cell. Exp Brain Res. 40: 383-392.

Table S1: Strength of connection (FLNe). (Target area is the injected area. while source area is the area containing the labeled neurons projecting to the target area).

Case	Monkey	Source area	Target area	FLNe
1	M81LH	V2	V1	7.38E-01
1	M81LH	V3	V1	7.97E-03
1	M81LH	V3A	V1	1.40E-03
1	M81LH	V4	V1	1.13E-01
1	M81LH	V4t	V1	1.41E-03
1	M81LH	LIP	V1	1.08E-03
1	M81LH	PIP	V1	9.60E-04
1	M81LH	DP	V1	1.71E-04
1	M81LH	STP	V1	1.75E-03
1	M81LH	PGa	V1	2.23E-04
1	M81LH	IPa	V1	6.86E-05
1	M81LH	FST	V1	8.54E-03
1	M81LH	MST	V1	1.27E-02
1	M81LH	MT	V1	5.74E-02
1	M81LH	TEO	V1	7.23E-03
1	M81LH	PERIRHINAL	V1	5.49E-04
1	M81LH	TE	V1	7.87E-03
1	M81LH	TH/TF	V1	3.36E-03
1	M81LH	CORE	V1	8.57E-06
1	M81LH	MB	V1	8.57E-06
1	M81LH	LB	V1	1.71E-05
1	M81LH	PBc	V1	1.37E-04
1	M81LH	8	V1	1.63E-04
1	M81LH	Pulvinar	V1	3.20E-03
1	M81LH	Amygdala	V1	1.27E-03
1	M81LH	LGN	V1	1.45E-02
1	M81LH	Claustrum	V1	1.62E-02
2	M85LH	V2	V1	7.16E-01
2	M85LH	V3	V1	5.93E-03
2	M85LH	V3A	V1	1.27E-03
2	M85LH	V4	V1	9.14E-02
2	M85LH	V4t	V1	2.75E-03
2	M85LH	7A	V1	2.11E-04
2	M85LH	LIP	V1	8.52E-04
2	M85LH	PIP	V1	2.86E-04
2	M85LH	DP	V1	7.50E-04
2	M85LH	STP	V1	2.15E-03
2	M85LH	PGa	V1	7.09E-04
2	M85LH	IPa	V1	3.00E-04
2	M85LH	FST	V1	7.31E-03
2	M85LH	MST	V1	3.98E-03
2	M85LH	MT	V1	4.97E-02
2	M85LH	TEO	V1	3.66E-02
2	M85LH	PERIRHINAL	V1	4.69E-03
2	M85LH	TE	V1	2.30E-02
2	M85LH	TH/TF	V1	5.55E-03
2	M85LH	CORE	V1	6.82E-06
2	M85LH	LB	V1	6.14E-05
2	M85LH	PBc	V1	1.09E-04
2	M85LH	8	V1	1.16E-04
2	M85LH	Pulvinar	V1	2.29E-03
2	M85LH	Amygdala	V1	1.68E-03
2	M85LH	LGN	V1	1.08E-02

Case	Monkey	Source area	Target area	FLNe
2	M85LH	Claustrum	V1	3.14E-02
3	M85RH	V2	V1	6.98E-01
3	M85RH	V3	V1	6.70E-03
3	M85RH	V3A	V1	1.55E-03
3	M85RH	V4	V1	1.34E-01
3	M85RH	V4t	V1	1.70E-03
3	M85RH	LIP	V1	9.39E-04
3	M85RH	PIP	V1	5.68E-04
3	M85RH	DP	V1	4.99E-04
3	M85RH	STP	V1	2.72E-03
3	M85RH	PGa	V1	1.01E-03
3	M85RH	IPa	V1	3.36E-04
3	M85RH	FST	V1	8.56E-03
3	M85RH	MST	V1	6.42E-03
3	M85RH	MT	V1	5.16E-02
3	M85RH	TEO	V1	3.49E-02
3	M85RH	PERIRHINAL	V1	1.73E-03
3	M85RH	TE	V1	1.28E-02
3	M85RH	TH/TF	V1	3.11E-03
3	M85RH	CORE	V1	1.53E-04
3	M85RH	MB	V1	1.98E-05
3	M85RH	LB	V1	3.95E-05
3	M85RH	PBc	V1	9.89E-05
3	M85RH	8B	V1	4.94E-06
3	M85RH	8	V1	3.26E-04
3	M85RH	Pulvinar	V1	2.85E-03
3	M85RH	Amygdala	V1	3.99E-03
3	M85RH	LGN	V1	6.67E-03
3	M85RH	Claustrum	V1	1.78E-02
4	M88RH	V2	V1	7.35E-01
4	M88RH	V3	V1	3.66E-03
4	M88RH	V3A	V1	5.11E-03
4	M88RH	V4	V1	7.01E-02
4	M88RH	V4t	V1	4.52E-03
4	M88RH	7A	V1	3.23E-04
4	M88RH	LIP	V1	1.51E-03
4	M88RH	PIP	V1	1.08E-04
4	M88RH	DP	V1	7.79E-04
4	M88RH	STP	V1	2.18E-03
4	M88RH	PGa	V1	8.33E-04
4	M88RH	IPa	V1	3.23E-04
4	M88RH	FST	V1	9.89E-03
4	M88RH	MST	V1	6.75E-03
4	M88RH	MT	V1	7.66E-02
4	M88RH	TEO	V1	2.52E-02
4	M88RH	PERIRHINAL	V1	2.12E-03
4	M88RH	TE	V1	2.59E-02
4	M88RH	TH/TF	V1	6.99E-03
4	M88RH	CORE	V1	5.38E-05
4	M88RH	MB	V1	5.38E-05
4	M88RH	LB	V1	1.08E-04
4	M88RH	PBc	V1	1.08E-04
4	M88RH	8	V1	2.69E-04
4	M88RH	Pulvinar	V1	2.39E-03
4	M88RH	Amygdala	V1	9.68E-04
4	M88RH	LGN	V1	1.28E-02
4	M88RH	Claustrum	V1	4.95E-03

Case	Monkey	Source area	Target area	FLNe
5	M121RH	V2	V1	6.70E-01
5	M121RH	V3	V1	9.27E-03
5	M121RH	V3A	V1	1.62E-03
5	M121RH	V4	V1	2.00E-01
5	M121RH	V4t	V1	6.85E-04
5	M121RH	LIP	V1	2.18E-03
5	M121RH	PIP	V1	1.88E-03
5	M121RH	DP	V1	1.81E-04
5	M121RH	STP	V1	1.66E-03
5	M121RH	PGa	V1	3.22E-04
5	M121RH	IPa	V1	1.41E-04
5	M121RH	FST	V1	7.30E-03
5	M121RH	MST	V1	1.87E-03
5	M121RH	MT	V1	5.09E-02
5	M121RH	TEO	V1	2.35E-02
5	M121RH	PERIRHINAL	V1	5.34E-04
5	M121RH	TE	V1	7.58E-03
5	M121RH	TH/TF	V1	2.58E-03
5	M121RH	PBc	V1	2.01E-05
5	M121RH	8	V1	3.12E-04
5	M121RH	Pulvinar	V1	4.06E-03
5	M121RH	Amygdala	V1	1.11E-04
5	M121RH	LGN	V1	1.13E-02
5	M121RH	Claustrum	V1	2.23E-03
6	M101LH	V1	V2	7.23E-01
6	M101LH	V3	V2	3.94E-02
6	M101LH	V3A	V2	1.10E-03
6	M101LH	V4	V2	1.75E-01
6	M101LH	V4t	V2	7.61E-04
6	M101LH	7A	V2	2.76E-06
6	M101LH	LIP	V2	7.72E-04
6	M101LH	VIP	V2	2.43E-04
6	M101LH	PIP	V2	5.68E-04
6	M101LH	DP	V2	5.16E-04
6	M101LH	PO	V2	3.86E-05
6	M101LH	STP	V2	1.19E-04
6	M101LH	PGa	V2	1.05E-04
6	M101LH	IPa	V2	7.45E-05
6	M101LH	FST	V2	2.23E-03
6	M101LH	MST	V2	4.99E-04
6	M101LH	MT	V2	3.60E-02
6	M101LH	TEO	V2	6.48E-04
6	M101LH	PERIRHINAL	V2	5.52E-04
6	M101LH	TE	V2	2.61E-03
6	M101LH	TH/TF	V2	1.96E-03
6	M101LH	MB	V2	8.27E-06
6	M101LH	LB	V2	2.76E-06
6	M101LH	8	V2	1.05E-04
6	M101LH	Pulvinar	V2	6.91E-03
6	M101LH	Amygdala	V2	3.92E-04
6	M101LH	LGN	V2	8.66E-04
6	M101LH	Claustrum	V2	5.15E-03
7	M101RH	V1	V2	7.66E-01
7	M101RH	V3	V2	4.24E-02
7	M101RH	V3A	V2	3.68E-03
7	M101RH	V4	V2	1.09E-01
7	M101RH	V4t	V2	9.62E-04

Case	Monkey	Source area	Target area	FLNe
7	M101RH	LIP	V2	1.45E-03
7	M101RH	VIP	V2	9.21E-05
7	M101RH	PIP	V2	2.84E-04
7	M101RH	DP	V2	8.17E-04
7	M101RH	PO	V2	2.00E-05
7	M101RH	STP	V2	1.60E-04
7	M101RH	PGa	V2	3.21E-05
7	M101RH	IPa	V2	4.01E-06
7	M101RH	FST	V2	2.31E-03
7	M101RH	MST	V2	1.21E-03
7	M101RH	MT	V2	4.03E-02
7	M101RH	TEO	V2	3.92E-03
7	M101RH	PERIRHINAL	V2	6.93E-04
7	M101RH	TE	V2	2.74E-03
7	M101RH	TH/TF	V2	2.44E-03
7	M101RH	MB	V2	4.01E-06
7	M101RH	8	V2	1.68E-04
7	M101RH	Pulvinar	V2	6.58E-03
7	M101RH	Amygdala	V2	5.05E-04
7	M101RH	LGN	V2	2.29E-03
7	M101RH	Claustrum	V2	1.12E-02
8	M103LH	V1	V2	7.57E-01
8	M103LH	V3	V2	1.02E-02
8	M103LH	V3A	V2	9.02E-04
8	M103LH	V4	V2	1.66E-01
8	M103LH	V4t	V2	1.82E-03
8	M103LH	7A	V2	1.56E-05
8	M103LH	LIP	V2	4.80E-04
8	M103LH	VIP	V2	5.73E-05
8	M103LH	PIP	V2	4.33E-04
8	M103LH	DP	V2	2.61E-05
8	M103LH	PO	V2	3.65E-05
8	M103LH	STP	V2	2.08E-04
8	M103LH	PGa	V2	3.02E-04
8	M103LH	IPa	V2	1.04E-04
8	M103LH	FST	V2	1.41E-03
8	M103LH	MST	V2	2.40E-04
8	M103LH	MT	V2	2.92E-02
8	M103LH	TEO	V2	1.01E-03
8	M103LH	PERIRHINAL	V2	4.07E-04
8	M103LH	TE	V2	4.98E-03
8	M103LH	TH/TF	V2	1.19E-03
8	M103LH	MB	V2	1.56E-05
8	M103LH	LB	V2	1.56E-05
8	M103LH	PBc	V2	5.21E-06
8	M103LH	8	V2	1.46E-04
8	M103LH	Pulvinar	V2	5.21E-03
8	M103LH	Amygdala	V2	1.94E-03
8	M103LH	LGN	V2	2.70E-03
8	M103LH	Claustrum	V2	1.40E-02
9	BB187LH	V1	V4	2.93E-03
9	BB187LH	V2	V4	3.24E-01
9	BB187LH	V3	V4	1.55E-02
9	BB187LH	V3A	V4	3.26E-05
9	BB187LH	V4t	V4	3.95E-02
9	BB187LH	LIP	V4	3.40E-03
9	BB187LH	DP	V4	7.00E-04

Case	Monkey	Source area	Target area	FLNe
9	BB187LH	PGa	V4	3.26E-05
9	BB187LH	IPa	V4	1.69E-03
9	BB187LH	FST	V4	6.22E-03
9	BB187LH	MST	V4	1.30E-04
9	BB187LH	MT	V4	8.06E-02
9	BB187LH	TEO	V4	2.81E-01
9	BB187LH	PERIRHINAL	V4	1.41E-02
9	BB187LH	TE	V4	1.38E-01
9	BB187LH	ENTORHINAL	V4	6.51E-04
9	BB187LH	TH/TF	V4	3.02E-02
9	BB187LH	8	V4	1.42E-03
9	BB187LH	Pulvinar	V4	1.14E-02
9	BB187LH	Amygdala	V4	1.87E-03
9	BB187LH	LGN	V4	3.42E-04
9	BB187LH	Claustrum	V4	4.57E-02
10	M121RH	V1	V4	7.70E-03
10	M121RH	V2	V4	3.24E-01
10	M121RH	V3	V4	4.13E-02
10	M121RH	V3A	V4	6.79E-05
10	M121RH	V4t	V4	7.86E-02
10	M121RH	7A	V4	1.56E-04
10	M121RH	LIP	V4	3.55E-03
10	M121RH	PIP	V4	8.82E-05
10	M121RH	DP	V4	1.43E-04
10	M121RH	STP	V4	3.80E-04
10	M121RH	PGa	V4	4.34E-04
10	M121RH	IPa	V4	5.77E-04
10	M121RH	FST	V4	1.05E-02
10	M121RH	MST	V4	1.63E-04
10	M121RH	MT	V4	6.28E-02
10	M121RH	TEO	V4	1.77E-01
10	M121RH	PERIRHINAL	V4	7.87E-03
10	M121RH	TE	V4	2.03E-01
10	M121RH	ENTORHINAL	V4	5.43E-05
10	M121RH	TH/TF	V4	1.86E-02
10	M121RH	INSULA	V4	6.11E-05
10	M121RH	9/46d	V4	6.79E-06
10	M121RH	9/46v	V4	3.39E-05
10	M121RH	8	V4	2.78E-03
10	M121RH	Pulvinar	V4	1.73E-02
10	M121RH	Amygdala	V4	1.89E-03
10	M121RH	LGN	V4	5.63E-04
10	M121RH	Claustrum	V4	4.00E-02
11	M123LH	V1	V4	1.63E-02
11	M123LH	V2	V4	3.98E-01
11	M123LH	V3	V4	1.36E-02
11	M123LH	V3A	V4	1.37E-04
11	M123LH	V4t	V4	8.53E-03
11	M123LH	7A	V4	3.90E-05
11	M123LH	LIP	V4	1.48E-03
11	M123LH	PIP	V4	7.81E-04
11	M123LH	DP	V4	3.90E-05
11	M123LH	STP	V4	6.93E-04
11	M123LH	PGa	V4	7.32E-04
11	M123LH	IPa	V4	1.87E-03
11	M123LH	FST	V4	1.31E-02
11	M123LH	MST	V4	7.81E-05

Case	Monkey	Source area	Target area	FLNe
11	M123LH	MT	V4	9.91E-02
11	M123LH	TEO	V4	2.16E-01
11	M123LH	PERIRHINAL	V4	6.38E-03
11	M123LH	TE	V4	1.23E-01
11	M123LH	ENTORHINAL	V4	5.86E-05
11	M123LH	TH/TF	V4	2.58E-02
11	M123LH	LB	V4	1.95E-05
11	M123LH	INSULA	V4	4.88E-05
11	M123LH	9/46v	V4	2.93E-05
11	M123LH	8	V4	1.99E-03
11	M123LH	Pulvinar	V4	1.10E-02
11	M123LH	Amygdala	V4	5.51E-03
11	M123LH	LGN	V4	1.17E-04
11	M123LH	Claustrum	V4	5.62E-02